1965

An investigation of continuous prestressed concrete structures

Ping-Chi Mao

AN INVESTIGATION OF
CONTINUOUS PRESTRESSED CONCRETE STRUCTURES

BY

PING-CHI MAO, 1934

A

THESIS

submitted to the faculty of the

UNIVERSITY OF MISSOURI AT ROLLA

in partial fulfillment of the requirements for the

Degree of

MASTER OF SCIENCE IN CIVIL ENGINEERING

Rolla, Missouri

1965

APPROVED BY

Jerry R Bayless (Advisor) Larry E Farmer

H-P-Pyron R.A. Schaefer

ABSTRACT

This thesis presents an analysis of the behavior of continuous prestressed concrete structures. From this analysis the governing equations for various types of geometry for prestressing cables are derived. The calculation of fixed-end moments due to the prestressing force using the equations derived is quite cumbersome, however, in order to simplify the calculations, design charts are developed. A cable with reverse curvature is analyzed using the design charts. It is shown that the fixed-end moments calculated by neglecting the effect of reverse curvature differ significantly from the fixed-end moments calculated by considering this effect. Hence the effect of reverse curvature should be considered for greater accuracy in design.

ACKNOWLEDGEMENT

The author of this thesis wishes to express his sincere appreciation to his advisor, Professor Jerry R. Bayless, of the Civil Engineering Department, for his guidance and counsel during the course of this investigation.

In addition, the writer is also indebted to Dr. L. E. Farmer, Assistant Professor of Civil Engineering, for his valuable suggestions and criticisms.

TABLE OF CONTENTS

LIST OF FIGURES

TABLE OF SYMBOLS

A-----Cross sectional area of the member.

b-----Width of beam.

b_1,b_2-Coefficients of distance from beam support to inflection points.

d-----Total sag of tendons.

d-----Depth of beam.

E-----Modulus of elasticity for concrete.

F-----Prestressing force.

f-----Unit stress in concrete.

H-----Horizontal component of prestressing force.

h-----Eccentricity of prestressing tendon.

I-----Moment of inertia of section.

I_x----Moment of inertia of variable sections.

K-----Friction coefficient of length effect.

k-----Moment coefficient.

L-----Span length.

ℓ-----length of tendon.

M-----Bending moment.

N-----Normal component of prestressing force.

R-----Radius of curvature.

R_b----Reaction at support B.

S-----Arc length.

W-----Uniform load.

w_1,w_2-Downward and upward uniform loads due to prestressing tendon.

x-----Horizontal ordinate of prestressing tendon.

y-----Vertical ordinate of prestressing tendon.

δ-----Deflection of tendon.

α-----Change in angle of tendon.

μ-----Coefficient of friction.

I. INTRODUCTION

Continuous structures are found as certain types of trusses, arches, rigid frames, fixed-end beams, propped cantilevers, as well as continuous beams and slabs which are quite common in building construction. Since continuous beams are stiffer than simple beams a smaller section can be used to carry a given load thus reducing the dead weight of the structure and attaining all the resulting economies. Recently, many ingenious methods of construction such as waffle slabs and the prestressed flat plates have evolved to take advantage of continuity.

As a rule in continuous structures, the negative moments at the points where the slab is continuous over the support are the maximum moments in the structure. This has led to many forms of section design or tendon placement. In cross-section design the members may have their depth increased by arching or by the use of haunches or a member of uniform depth may be widened from the point of inflection to the support. Two or more prestressing tendons may be acting at the same elevation over the support or additional short tendons may be added to increase both flexural and shear resistance.

From the standpoint of serviceability, prestressed concrete structures are more suitable for longer spans than conventionally reinforced structures. They normally do not crack under working loads, and whatever cracks

develop under overloads will close as soon as the load is removed unless the overload is excessive. Under dead loads, deflections and moments are reduced by the cambering effect of prestressing. Among the many advantages, the most important is the control of slab or beam moments. It is possible to control very precisely the magnitude of the bending moments by controlling the prestress force and the geometry of the tendon. The calculation of fixed-end moments due to the prestressing force of practical cable profiles is quite cumbersome. An attempt has been made in this investigation to simplify this procedure.

This work contains three main parts. In the first part, the concepts related to the behavior of continuous prestressed concrete structures are reviewed and applied; in the second part, the equations for fixed-end moments are derived; in the third part, design charts are developed.

II. REVIEW OF LITERATURE

Although prestressed concrete was not practical in general applications as late as 1933, the basic principle of prestressed concrete was conceived almost as early as that of reinforced concrete. P. H. Jackson [1], an engineer of San Francisco, California, was the first to advance an accurate conception of prestressing. Around 1886, he obtained patents for tightening steel tie rods in artificial stones and concrete arches which served as floor slabs.

In 1888, C. E. W. Doehring [1] of Germany suggested prestretching steel reinforcement in a concrete slab in order to promote simultaneous rupture of these two materials of distinctly different extensibilities. These applications were based on the conception that concrete, though strong in compression, was quite weak in tension, and prestressing the steel against the concrete would put the concrete under compressive stress which could be utilized to counterbalance any tensile stress produced by dead or live loads. J. Mandl [2] of Germany made a theoretical treatment of design of prestressed concrete in 1896, only two years after Edmond Coignet and Napoleon de Tedesco [2] developed the presently accepted theory of reinforced concrete in France. The theory of prestressed concrete was further developed by M. Koenen [2] of Germany in 1907. F. Dischinger [2], in 1928, first used prestressing

in major bridge construction---a deep-girder type in which prestressing wires were placed inside the girder but were not bonded to the concrete. About that time, prestressed concrete began to acquire importance, though it did not actually come to the fore until about 1945.

Most of the previously published methods of analysis for continuous prestressed structures having draped cables are based on the fundamental concepts which are described in the following paragraphs.

It is obvious that there are no bending moments in a cable that hangs between two supports (Figure 1). Also, there is no shear as occurs in a beam, and the loads are transferred directly to the supports. The tensile force in the cable is a function of the span, the load, and the profile. From simple statics, it can be seen that the tensile force, F, times the deflection of the cable, δ, is equal to $\frac{wL^2}{8}$, where L is the span and w is the weight of the cable in pounds per foot.

Next consider a uniform load hung from a cable at some distance below it (Figure 2). The uniform load could be a deep concrete slab. There is no bending in the slab since it is uniformly supported. If the uniform load is made large enough, the cable will remain essentially in a parabolic curve, even though a moving live load may be superimposed.

giving the cable

The uplift force of the cable equals the supported uniform load and the gravity loads are transferred to the cable supports.

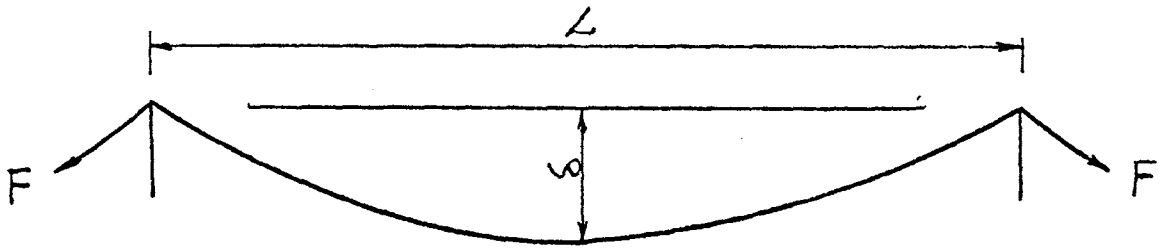

Fig. 1. Parabolic Draped Cable.

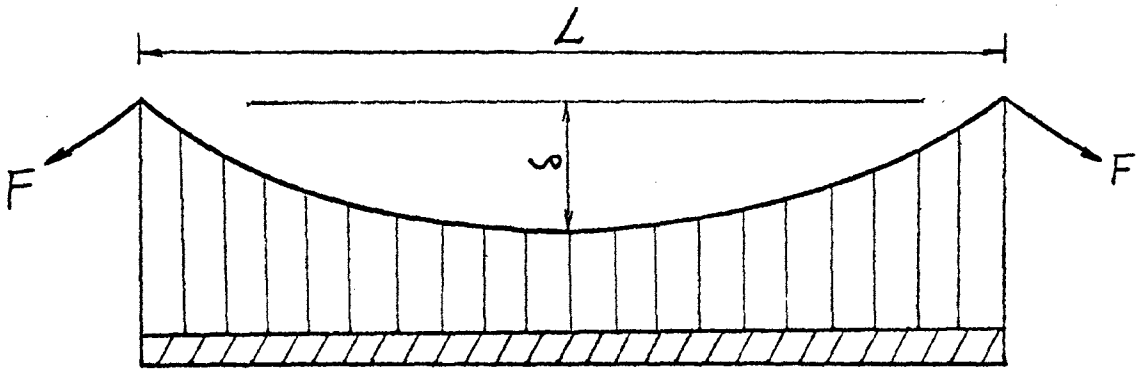

Fig. 2. Uniform Load Hung From A Cable.

Figure 3 shows a cable hung with small deflections from several supports, namely, the columns of a building. If the cable were enclosed in concrete, but not bonded, it would be possible to put a tensile force in the cable without changing radically the position of the cable, thus giving the cable an uplift force. If the cable tension is

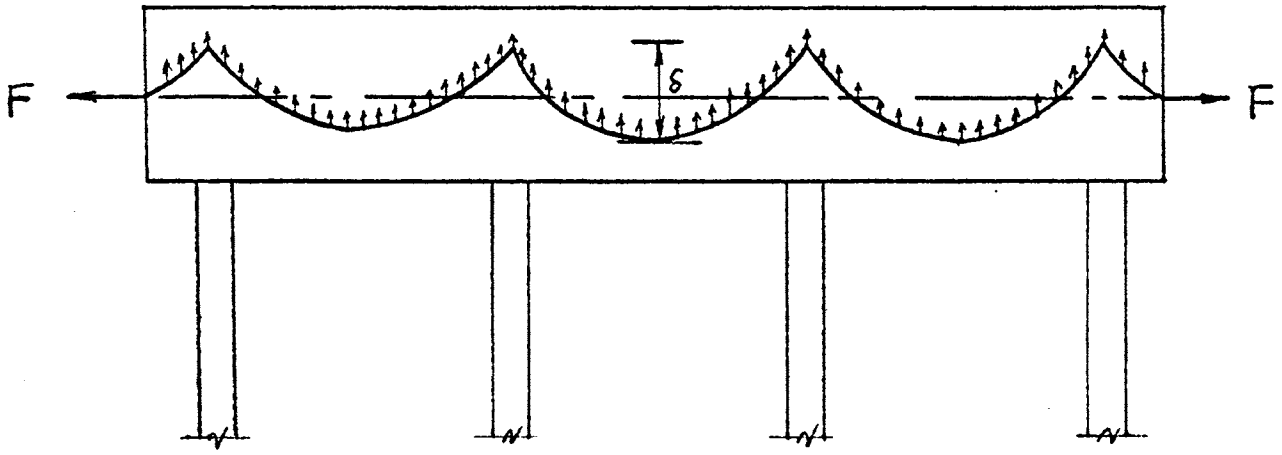

Fig. 3. Ideal Profile of Cable.

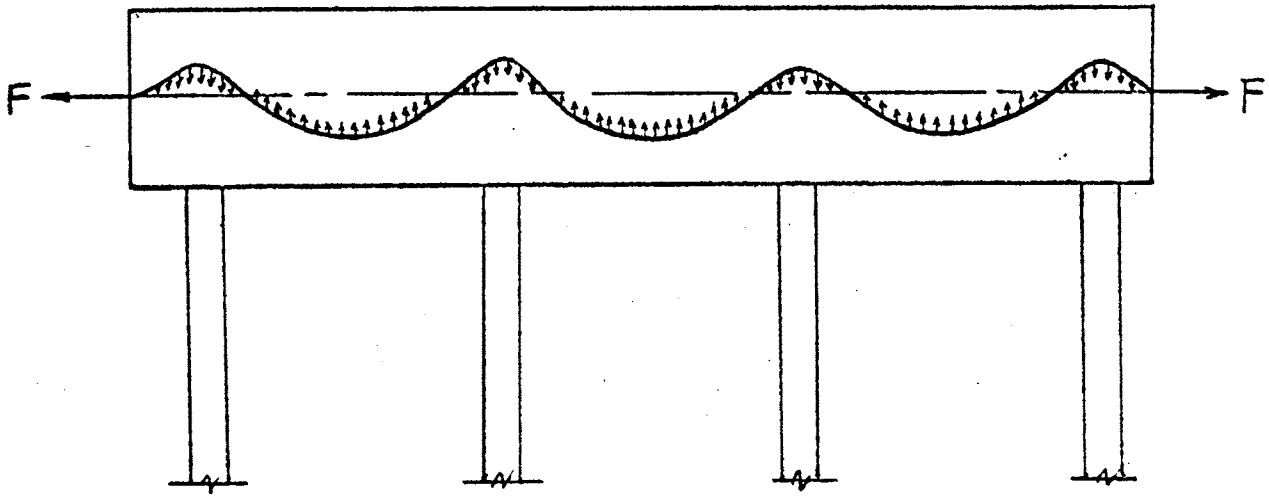

Fig. 4. Actual Profile of Cable.

adjusted so that the uplift force of the tendon is equal to the downward load of the structure, the concrete would have no bending stresses, and therefore no vertical deflection. Accordingly, the stress in the concrete would be F/A, where A is the cross-sectional area of the member, if the cables are anchored to the concrete by end plates. If the cables were anchored on each end to supports external to the building, there would be no stress in the concrete. The concrete has no deflection under this condition of loading and the reactions of the downward loads would be transferred directly into the reactions or the columns.

From a practical point of view, it can be seen that it is impossible to place the continuous tendons in the configuration in Figure 3. They must be placed in smooth continuous curves. Figure 4 shows a tendon as it is actually placed in practice. These curves are continuous parabolas exerting upward forces where concave upward, and downward forces where concave downward.

An attempt has been made in this thesis to apply the applicable theories to the actual profile of tendons and to derive the corresponding equations for fixed-end moments. From these equations design charts were developed for rapid design and the effect of reversal of curvature is determined.

III. BEHAVIOR OF CONTINUOUS PRESTRESSED CONCRETE STRUCTURES

In this section important concepts, such as cable geometry, the idealized cable structure, the line of thrust concept and loss of prestress due to friction as related to the behavior of continuous prestressed concrete structures, will be analyzed.

A). Cable geometry. It is obvious that there is no bending in a cable as it hangs between two supports. Figure 5-a shows a uniformly loaded cable with a parabolic profile. The tensile force in the cable is a function of the span, the vertical load, and the profile of the cable. The relation among them can be calculated as follows:

Let F = the tensile force in the cable

w = the uniform vertical load on the cable

L = span

The coordinates of the cable at any point are x and y. Also, the weight of the cable is considered negligible compared to the applied load.

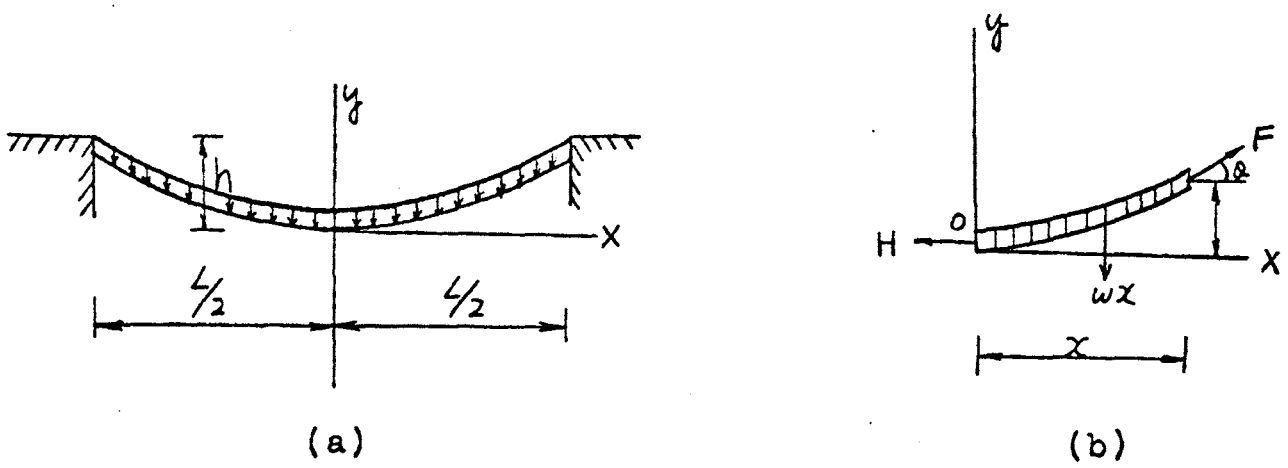

Fig. 5. Parabolic Cable Profile

Considering the force acting on the cable at x, which makes an angle α with the horizontal, and resolving the forces horizontally and vertically, Figure 5-b, the following equations are derived:

$$\sum F_y = 0 : F \sin\alpha - wx = 0$$

$$F = \frac{wx}{\sin\alpha}$$

$$\sum F_x = 0 : F \cos\alpha - H = 0$$

$$F = \frac{H}{\cos\alpha}$$

where F_y and F_x mean vertical and horizontal component respectively.

Hence, $\frac{wx}{\sin\alpha} = \frac{H}{\cos\alpha}$

$$\frac{wx}{H} = \frac{\sin\alpha}{\cos\alpha} = \tan\alpha = \frac{dy}{dx}$$

Differentiating with respect to dx,

$$w = H \frac{d^2y}{dx^2}$$

Integrating w, with the origin placed at the center of the span of total length L, then

$$y = \frac{w}{2H} x^2 + C_1x + C_2$$

With the boundary conditions $\frac{dy}{dx} = 0$ and $y = 0$ at $x = 0$, it is seen that $C_1 = 0$ and $C_2 = 0$. Also with $y = h$ at $x = \frac{L}{2}$, where h is the sag, the value of H is obtained as

$H = wL^2/8h$,

Where α is very small, $H = F \cos \alpha \cong F$; therefore,

$$F = \frac{wL^2}{8h} \qquad \text{----------(1)}$$

The assumption that the horizontal component is equal to the tensile force in the wires usually results in an error of less than 0.3 percent for the conditions encountered in prestressed concrete construction.

B). Idealized cables. An idealized cable supported by a concrete beam or slab is one in which the cable is placed as shown in Figure 3. It is impossible to place continuous tendons in this manner since they must be placed in smooth continuous curves. Smooth curves are necessary to reduce the friction in the stressing operation. Figure

4 shows a tendon as it is actually placed in the field. It can be seen that there are downward forces in the area over the support similar to the upward forces shown in Figure 3. The computations for an idealized cable will be illustrated by the following example.

A flat plate structure is sketched in Figure 6. It has a column spacing of 25 feet, a cantilever of 5 feet and a slab thickness of 10 inches. Although this example is concerned with a column strip of a slab, the design method presented applies to continuous beams as well as to slabs.

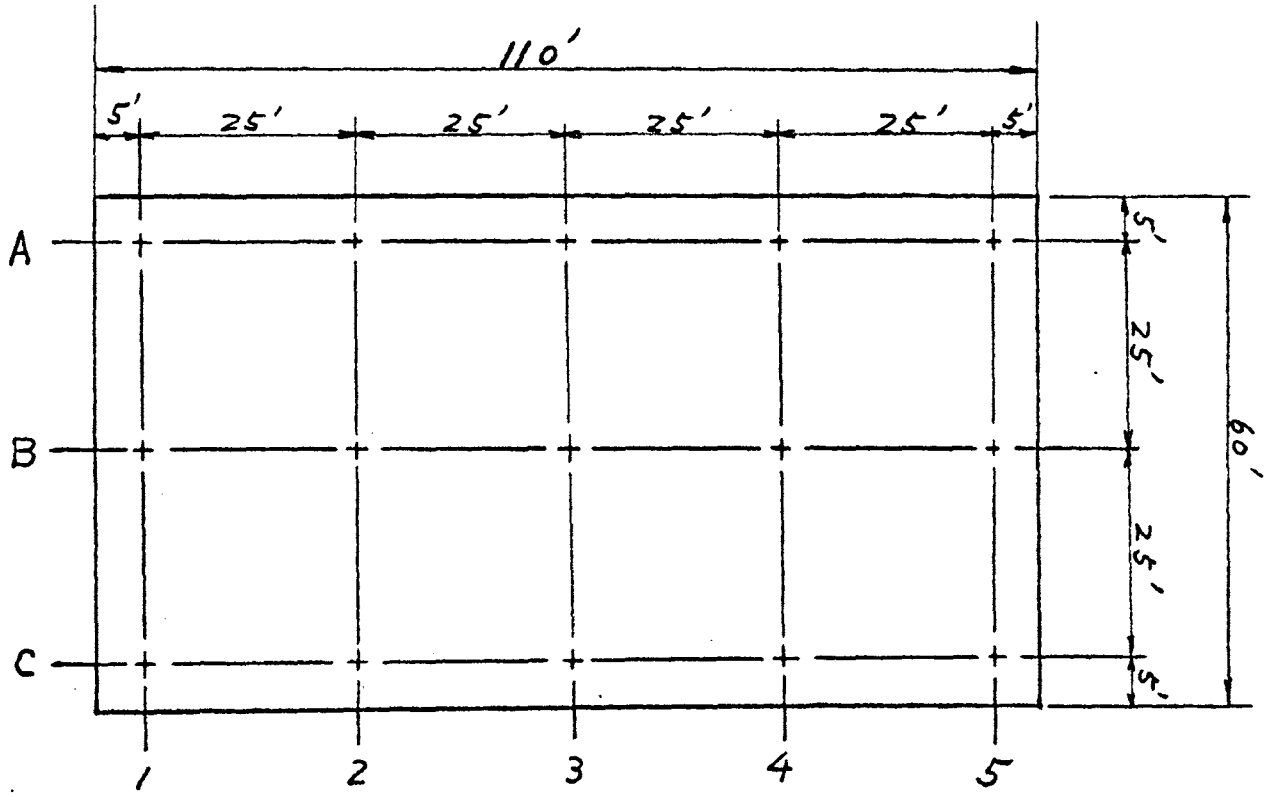

Fig. 6. A Flat Plate Structure.

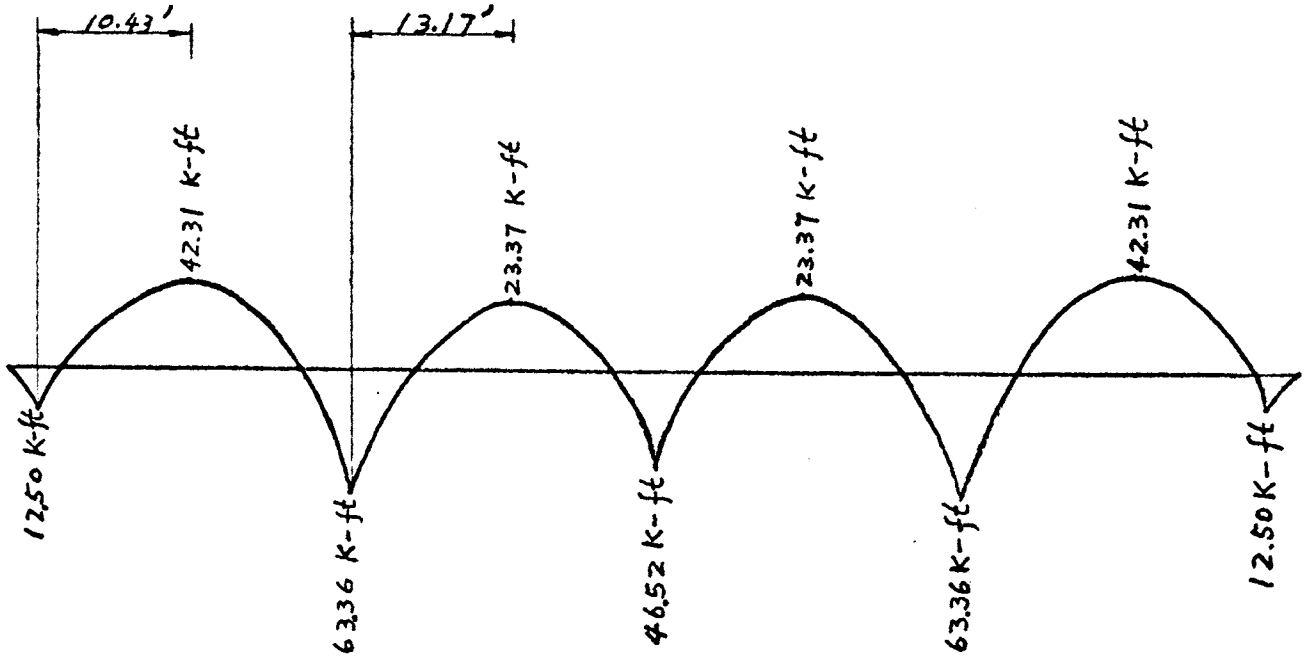

Fig. 7. Moment Curves for Unit Uniform Load.

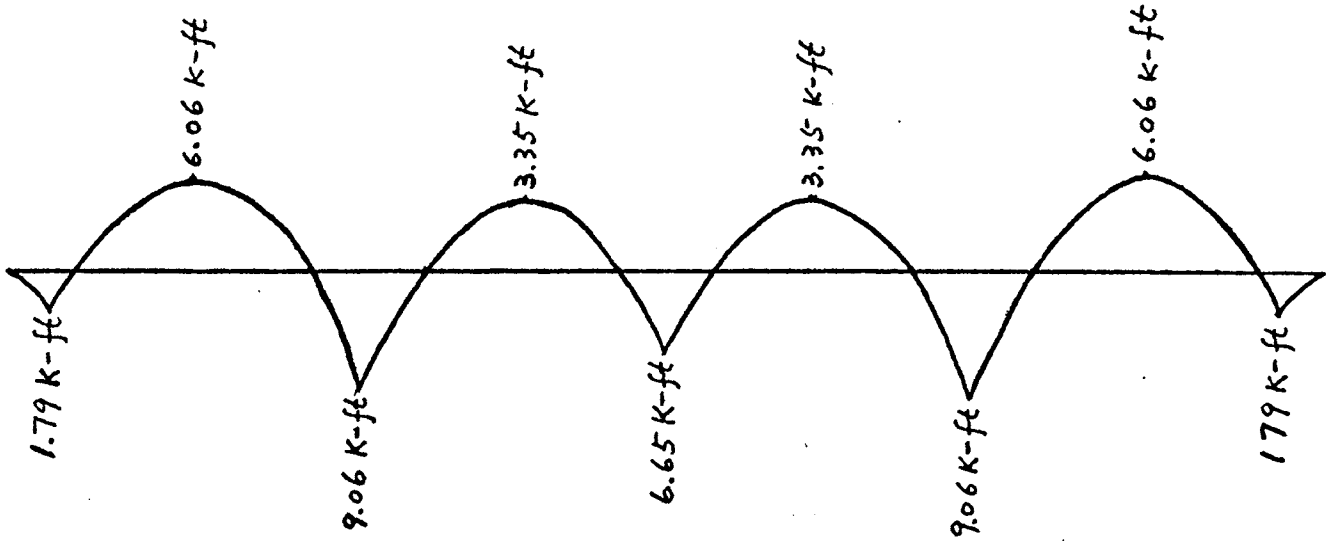

Fig. 8. Moment Curves for Uniform Dead Load of 143 psf.

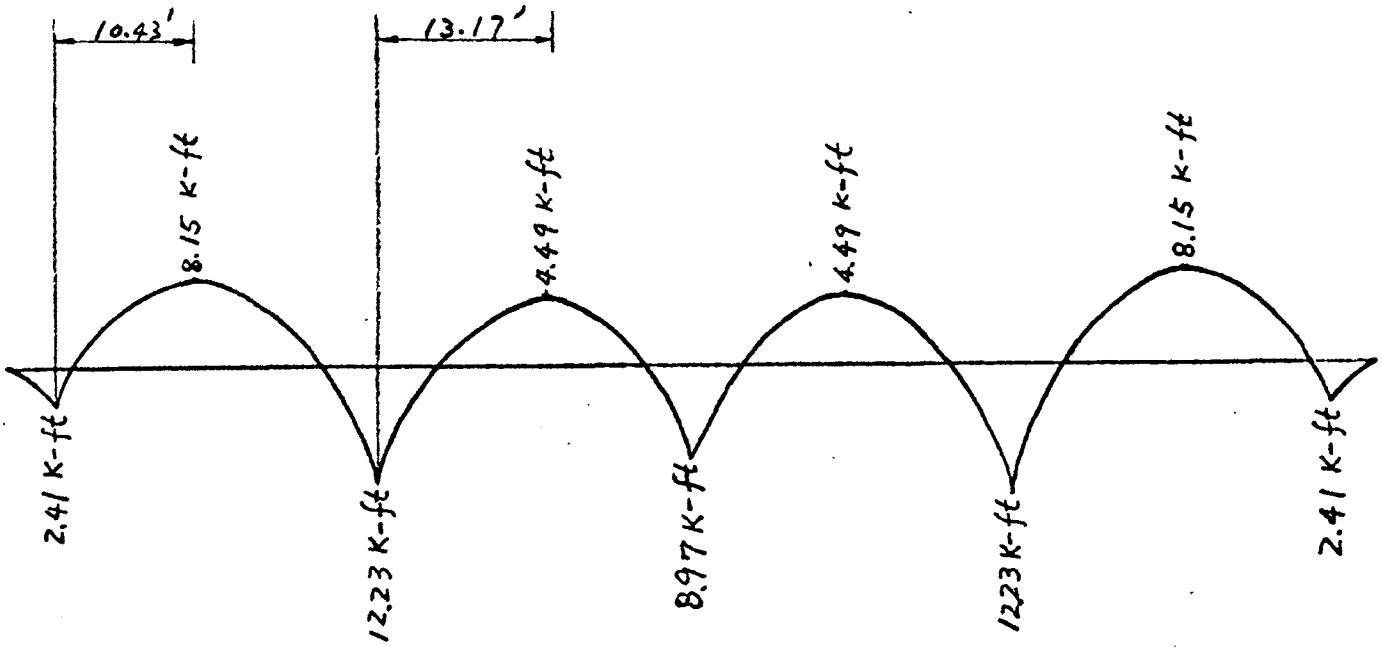

Fig. 9. Moment Curves for Uniform Dead and Live Loads of 193 psf.

In this example, the following loads are assumed: a partition load of 10 psf, a ceiling load of 8 psf, a 10 inch concrete slab at 125 psf, and a live load of 50 psf. Let it be desired to design the slab to be level under dead load.

Using the moment distribution procedure, the moments were found for a one foot wide strip of the slab along the column line and spanning the long direction. Figure 7 shows the resulting moment diagram for a unit uniform load, and Figures 8 and 9 show the moment diagram resulting from the uniform dead load of 143 psf. and the uniform dead and live load of 193 psf.

In Figure 10, a cable location was plotted with ordinates of the cable in direct proportion to the dead load moment curve. The maximum eccentricity, h = 0.30 ft., was placed at the point of maximum moment. The tendon as shown in Figure 10 is referred to as a concordant cable which is coincident with the line of thrust. It is also possible to plot a nonconcordant cable and determine the effects of the secondary moments caused by the eccentricity of the tendon with the line of thrust. Generally, it is not necessary to know the secondary moments, since only the total moments produced by the cable are required.

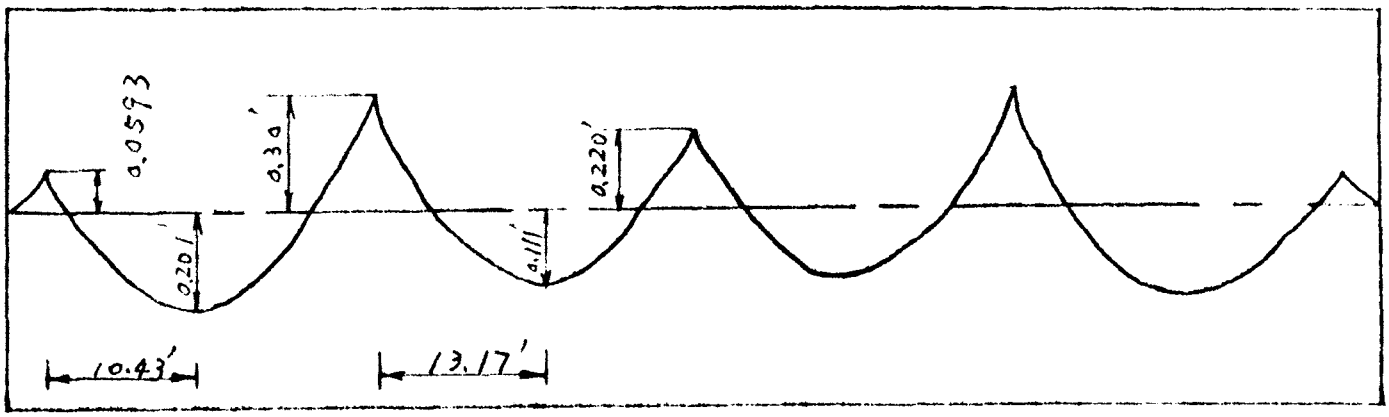

Fig. 10. A Concordant Cable Location for the Column Strip.

The following analysis shows that no secondary moments exist in this instance. The moment curve due to the prestressing force is drawn in Figure 11 in terms of F, the prestressing force. From Eq. 1 the upward force w in kip per foot

of span is equal to $8F\delta/L^2$, where δ is equal to 0.3707 feet (see Figure 11). Hence, the uniform upward load w is 0.00476F which is in direct proportion to the uniform downward load. If this uniform load is placed on the structure and the fixed-end moments are calculated and balanced, the moments shown in Figure 12 result. For no deflection due to dead load, the moments due to prestressing should equal dead load moments, and this can be accomplished with the proper choice of F. Thus, no secondary moments are induced into the slab by the concordant tendon force. If any position other than a concordant position were used, secondary effects would be evident in the balanced moments.

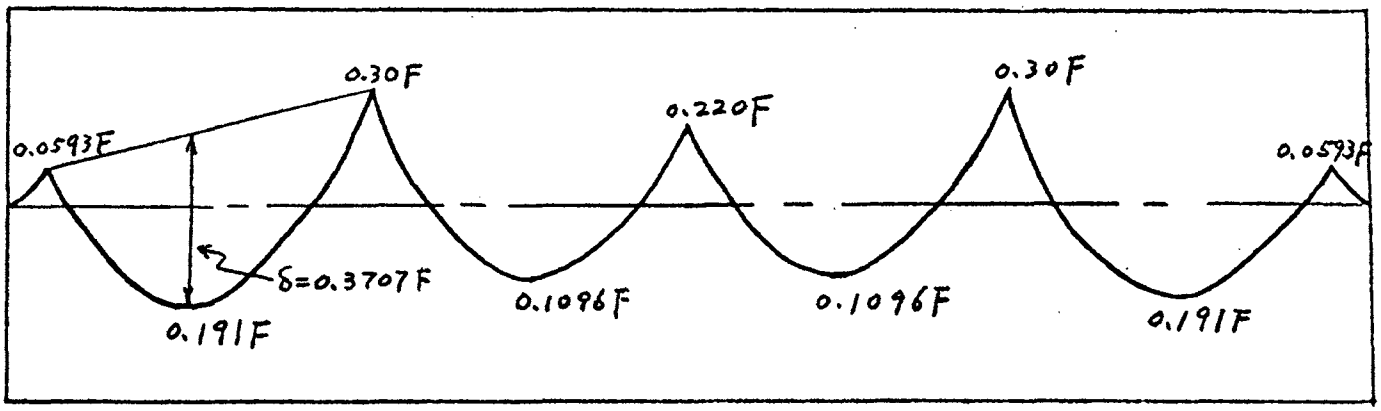

Fig. 11. Moment Curve Due to Prestressing Force.

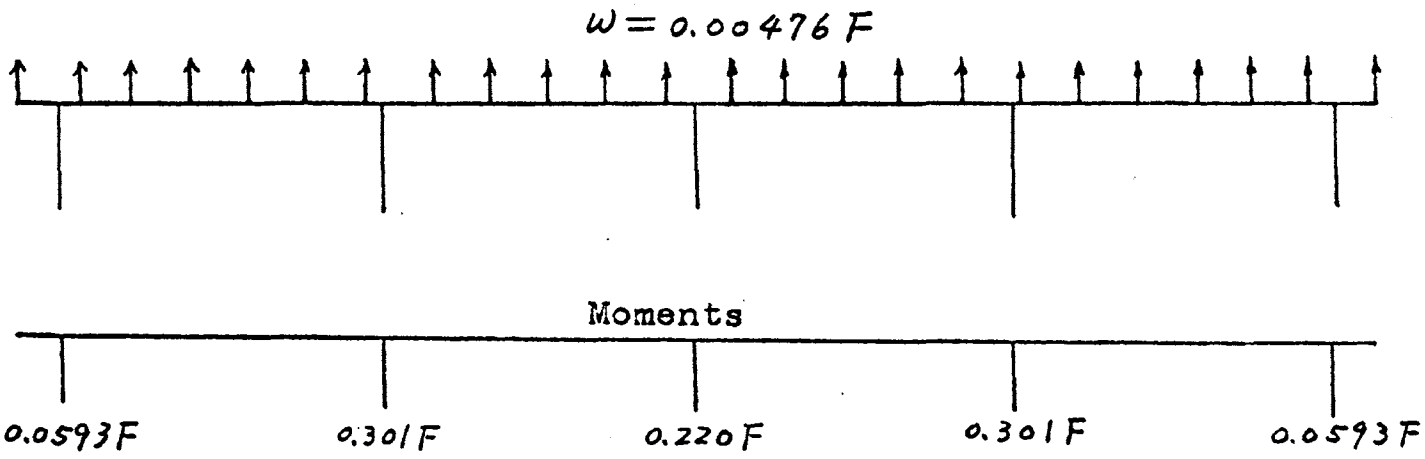

Fig. 12. Balanced Moments Due to Upward Load w = 0.00476F.

The dead load moments due to downward loads are set equal to the moments due to upward loads and the prestress force is calculated directly. Hence, 0.30F = (63.36) (0.143) where 0.143 is dead load in kip/ft. Therefore, F = 30.2 kips. Since the downward loads equal the upward loads, there is no bending, and the stress in the slab is F/A. In Figure 13, the moment diagram of the dead load has been superimposed on the moment diagram of the tendon load. It can be seen that the moments are equal and opposite in sign. Therefore, the bending stresses are zero and the only existing stress is the F/A stress.

In Figure 14, the moment diagram due to the dead load plus the live load has been superimposed on the moment diagram due to the tendon load. The moment due to the dead load plus the live load equals the moment of the unit load times 0.193 kips per foot. The algebraic sum of the bending moments along the slab gives the residual moment that must be resisted by the concrete. The tensile

stresses which would result in the concrete due to the residual bending moments are generally overcome by the axial compression, F/A, which results from self-anchoring the cable. In this example, referring to Figure 14, the residual moment at the first interior column is

12.23 - 9.06 = 3.17 k-ft.

$$\text{Hence, } f_c = \frac{F}{A} \pm \frac{MxY}{I} = \frac{(30.2)(1000)}{120} \pm \frac{(3.17)(1000)(12)(5)}{1000}$$

= 252 ± 190 psi, where compression is considered to be positive.

Therefore, for the top fiber f_c = 62 psi, and for the bottom fiber f_c = 442 psi.

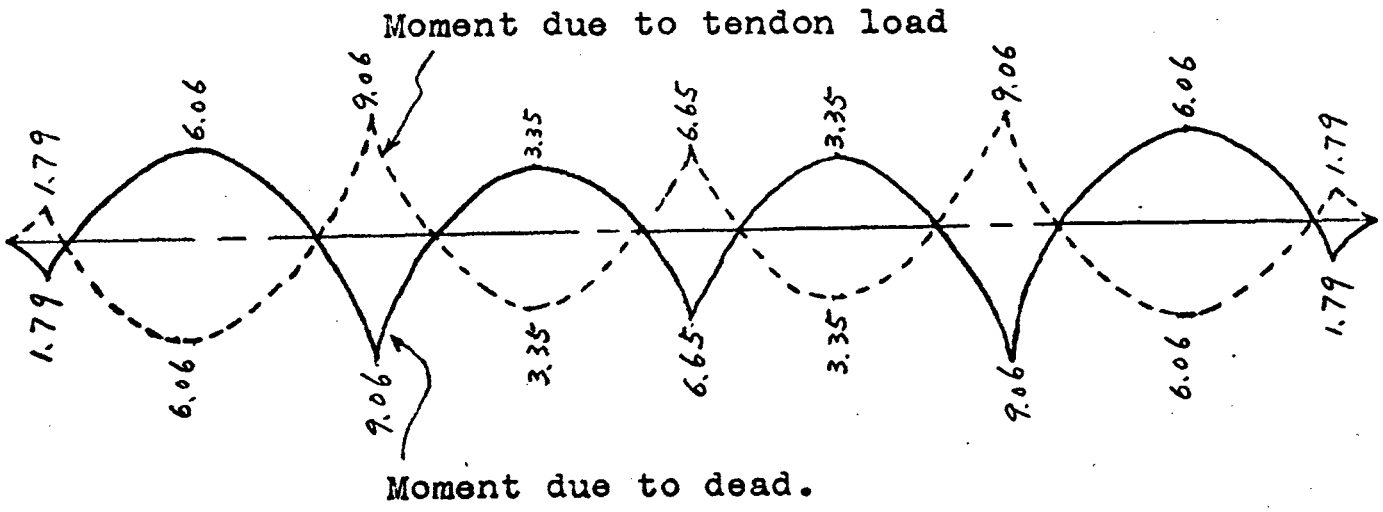

Moments shown are in the units of kip-ft.

Fig. 13. Superimposed Moment Diagrams for Tendon and Dead Loads.

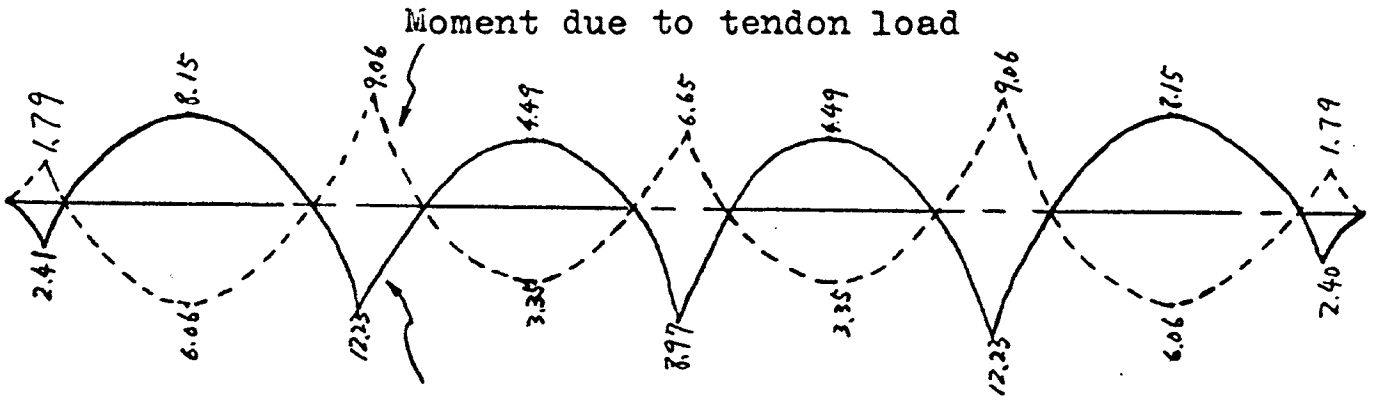

Moments shown are in the units of kip-ft.

Fig. 14. Dead Load and Live Load Moment Diagram Superimposed on Tendon Load Moment Diagram.

C). Line of thrust concept. In the analysis of a prestressed structure without external loads, the prestress force F may be thought of as a compressive thrust, producing only uniform direct compressive stress over the cross section when the thrust coincides with the center of gravity of the concrete section, but producing both direct compressive stresses and bending stresses when it is eccentric with respect to the center of gravity of the concrete section. Thus the profile of the prestressing element represents the line of thrust of a simply-supported prestressed structure. If the center of gravity of the concrete section is considered as the base line, the profile becomes the moment diagram to the scale of 1/F, or it may be regarded as a true moment diagram for a force F equal to unity. Since in practically all cases

eccentricities are small in comparison to span length, no distinction needs to be made between F and its horizontal component as these are nearly equal.

In continuous structures, when prestressing tendons are placed eccentrically with respect to the centroidal axis of the cross section, additional moments due to continuity are created. If the profile of the prestressing steel has been determined or assumed, the entire beam may first be regarded as if it had no supports. The moment diagram produced by the eccentricity of prestress is Fe, where F is the prestress force and e is the distance from the centroid of the section to the prestressing tendon. Since F is considered to be constant throughout the member, the moment diagram is given by the eccentricity curve plotted to some suitable scale. If the member should possess a curved axis, it is only necessary to plot the moment diagram by measuring the eccentricity from the curved center of the gravity line of the concrete section instead of from a straight base line. From this moment diagram, the corresponding shear diagram can be plotted. The equivalent vertical load on the beam necessary to produce the moment and shear diagram can then be computed. With this load acting on the continuous member as it is actually supported, and including any singular moments such as might occur at the ends of the beam due to the eccentricity of center of gravity

of steel area at the end, the resulting moments can be computed and plotted. Dividing the ordinates of the resulting moment diagram by the force F produces a diagram which deviates linearly from the profile of the center of gravity of the prestressing steel area, and this diagram has the same shape as the center of gravity line of the steel area. This diagram gives the actual thrust profile representing the total effect of prestressing for the continuous structure. For horizontal members, when the thrust line is above the upper kern limit of the concrete section, the eccentricity produces tension in bottom fibers; when it is below the lower kern limit of the concrete section, it produces tension in the top fiber of the member.

In considering the effects of external loads, the moments due to the external loads are evaluated by the usual methods, such as moment distribution. The moment diagram for the external load effect is drawn and the ordinates are divided by the force F. The result is the thrust profile due to external loads, and when ordinates are added algebraically to those for the prestress effect, the line of thrust for the combined load is obtained. A continuous prestressed concrete beam will be analyzed to illustrate the procedure described above.

A continuous prestressed concrete beam with bonded tendons is shown in Figure 15. Assume a prestressing

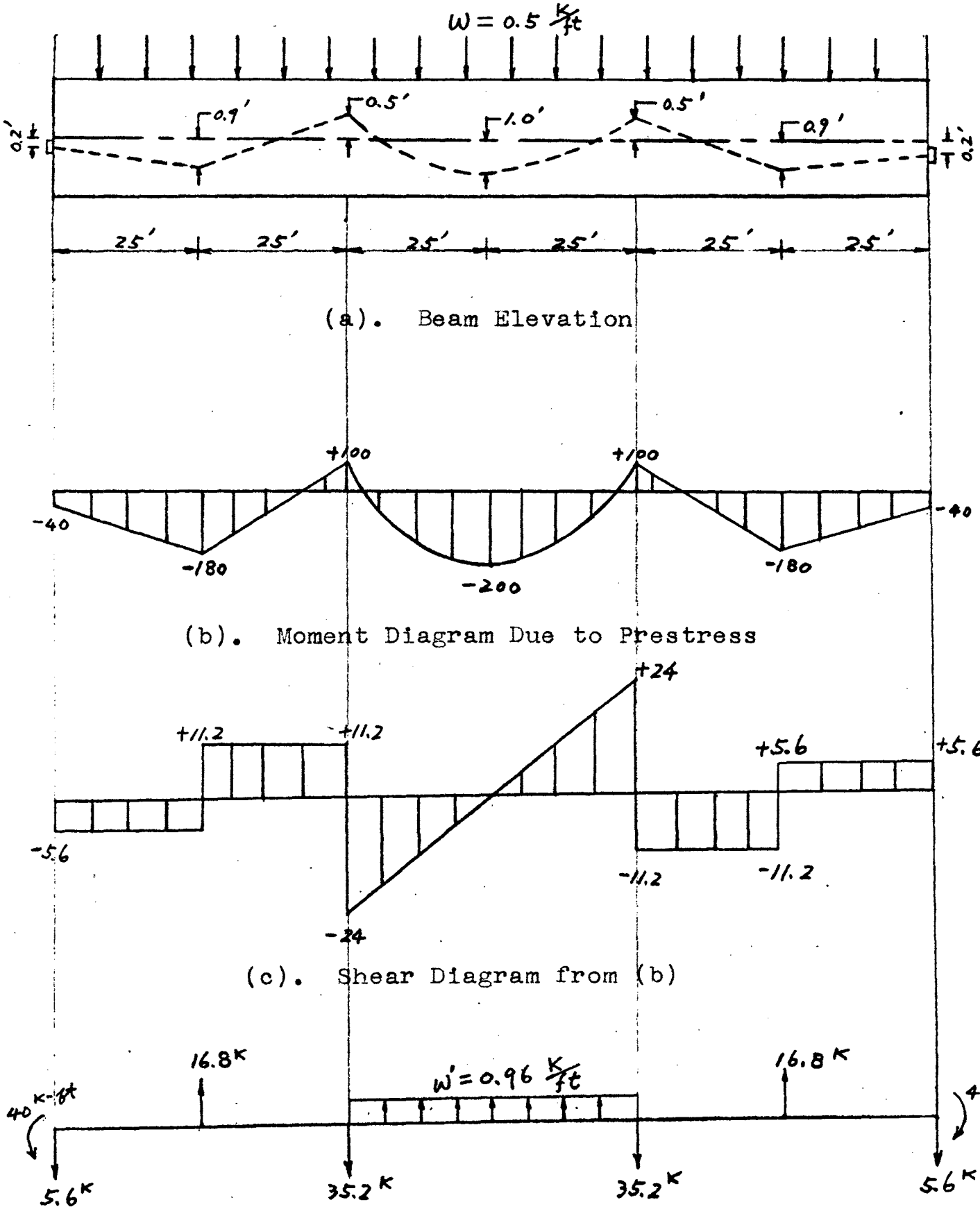

(a). Beam Elevation

(b). Moment Diagram Due to Prestress

(c). Shear Diagram from (b)

(d). Forces from Tendon on Concrete

Fig. 15. Computation of Equivalent Loading Diagram Due to Prestress.

force of 200k and a uniform external load w = 0.5 kips per foot on all spans.

The moment diagram for the entire continuous beam produced by the eccentricity of prestress is shown in Figure 15-b. When the center of gravity line of the steel area is above the center of gravity line of the concrete section, the eccentricity produces a positive moment; when it is below the center of gravity line of the concrete section, it produces a negative moment. From Figure 15-b, the corresponding shear diagram is computed and shown in Figure 15-c.

In Figure 15-d, the loads necessary to give the shear and the moment of Figure 15-b and Figure 15-c are computed. This is the equivalent loading produced by the steel on the concrete. The final moments at the supports due to prestressing are found from moment distribution and are given in Figure 16. Values of M/F at the supports are evaluated, and by a linear transformation, the line of thrust due to prestressing is plotted in Figure 17.

The moment diagram due to external loading is found from moment distribution and is plotted in Figure 18. Values obtained by dividing the moments due to external loads by the prestressing force are the ordinates of the line of thrust which are plotted in Figure 19. When the

two thrust lines shown in Figures 17 and 19 are added algebraically, the final location of the thrust profile for all effects is obtained (Figure 20).

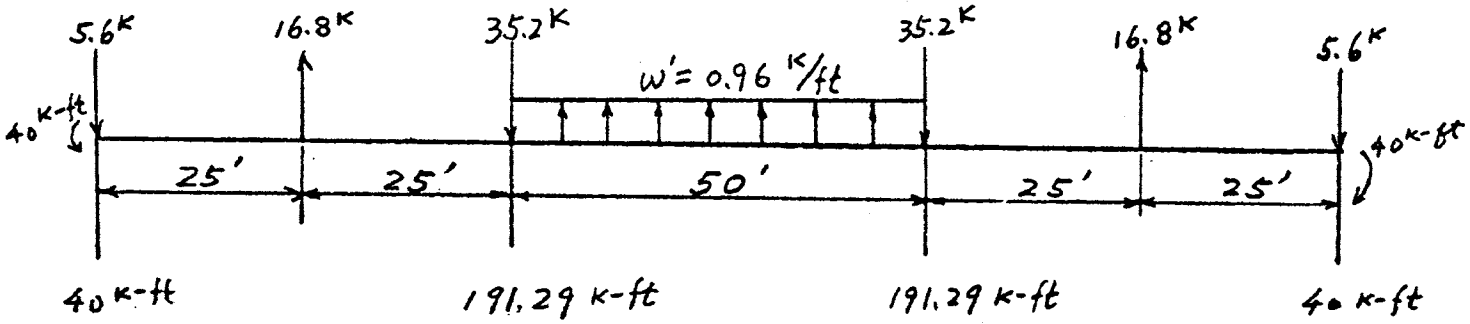

Fig. 16. Final End moments for Loading Shown in Fig. 15-d.

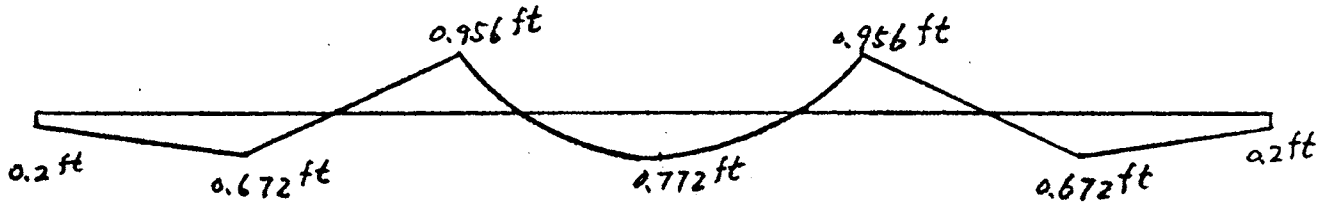

Fig. 17. Line of Thrust for Loading Shown in Fig. 15-d.

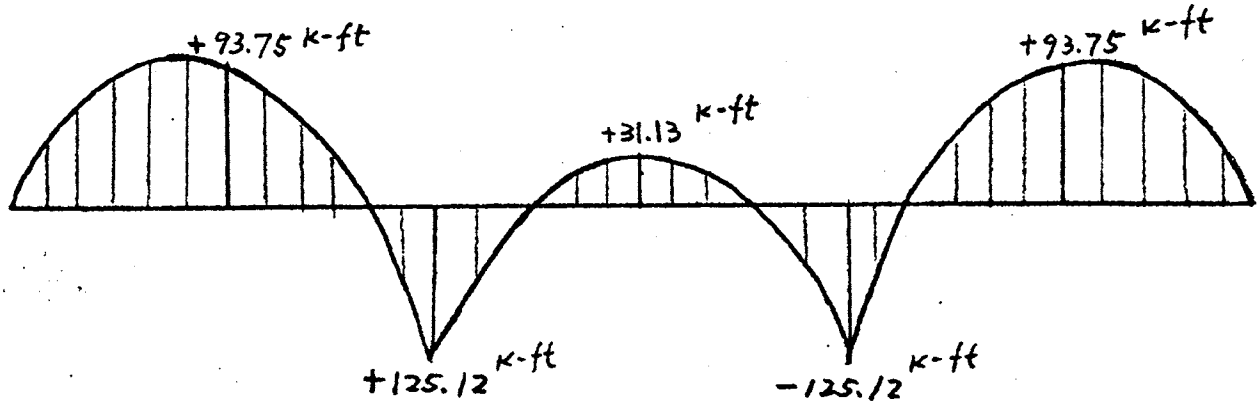

Fig. 18. Moment Diagram for External Loading Shown in Fig. 15-a.

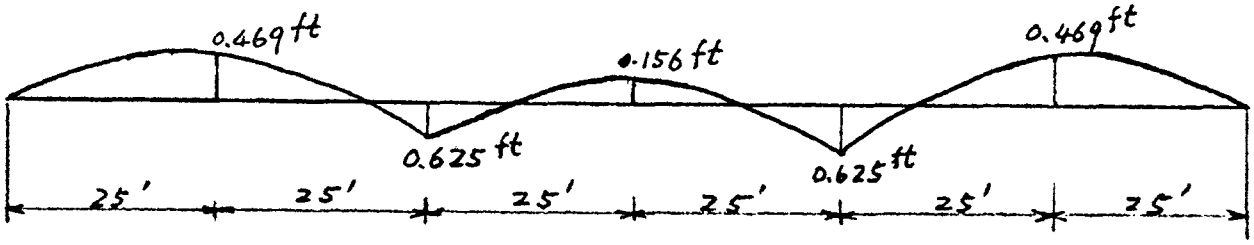

Fig. 19. Line of Thrust for External Loading Shown in Fig. 15-a.

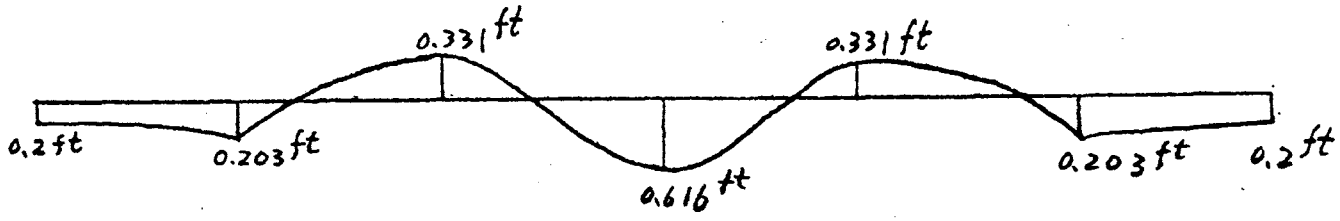

Fig. 20. Final Line of Thrust for the Beam Shown in Fig. 15..

D). Loss of prestress due to friction. One of the important problems in the design of continuous prestressed concrete structures is the friction between the prestressing tendon and the concrete. In post-stressing the tendon is tensioned after the concrete has hardened and while jacking the tendon there is some friction created. In order to make the moments due to the prestressing force opposite to those caused by the acting loads, reversed curves are used. The basic theory of frictional loss of a cable around a curve,(Fig. 21-a) is discussed below.

The diagram shows the frictional force along an infinitesimal length of tendon, dx, with a radius of

curvature R and angle $d\alpha$ The normal component dN is given by:

$$dN = F\frac{d\alpha}{2} + F\frac{d\alpha}{2} + dF\frac{d\alpha}{2}, \text{ or } dN = Fd\alpha$$

where the higher order term $dFd\alpha$ is neglected.

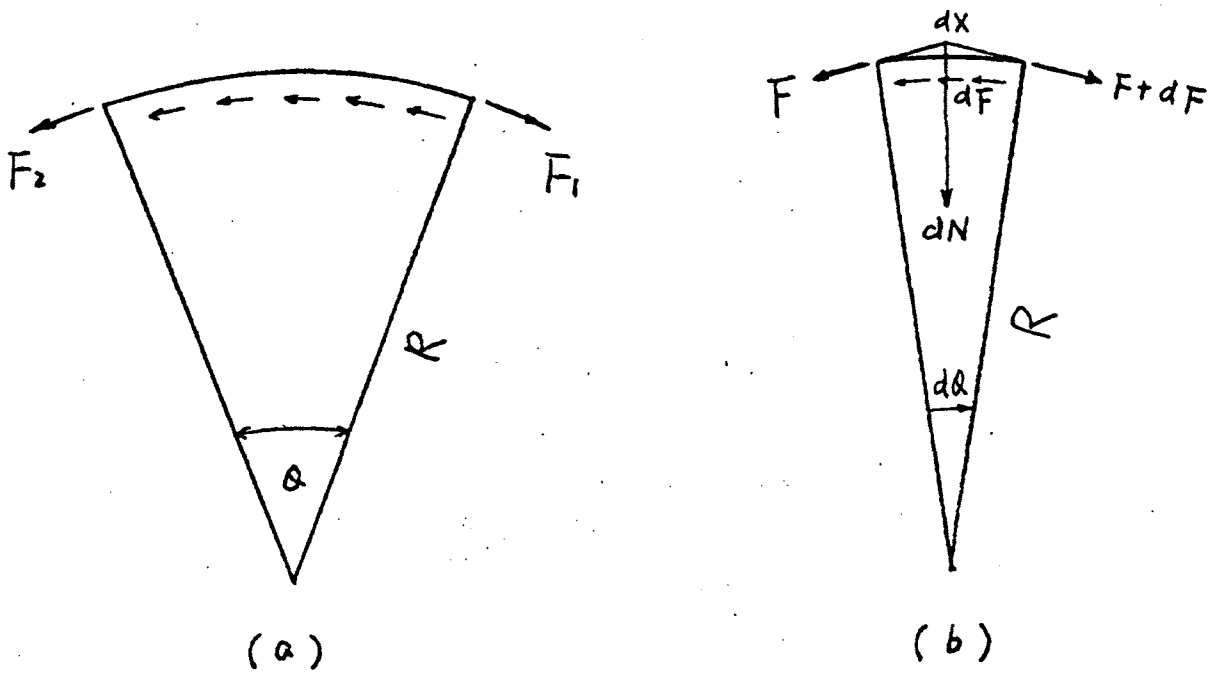

Fig. 21. Frictional Loss of a Curved Cable.

The amount of frictional loss dF on the length dx is given by dN times a coefficient of friction μ, thus,

$$dF = \mu dN = \mu F d\alpha$$

$$\frac{dF}{F} = \mu d\alpha$$

Integrating both sides of this equation,

$$\left[\ln F\right]_{F_1}^{F_2} = \left[\mu\alpha\right]_0^{\alpha}$$

$$\ln F_2 - \ln F_1 = \mu(0 - \alpha)$$

$$\ln\frac{F_2}{F_1} = -\mu\alpha \quad \text{or} \quad \frac{F_2}{F_1} = e^{-\mu\alpha}$$

$$F_2 = F_1 e^{-\mu\alpha} \text{ ----------(2)}$$

Equation (2) can be applied to compute the frictional loss due to wobble or length effect by replacing $\mu\alpha$ with KL, where K is a coefficient of wobble or length effect. The combined effedt of curvature and length is found by adding the individual effects.

$$\ln\frac{F_2}{F_1} = -\mu\alpha - K\ell$$

$$F_2 = F_1 e^{-(\mu\alpha + K\ell)} \text{ ----------(3)}$$

But $e^{-(\mu\alpha + K\ell)} = 1 - (\mu\alpha + K\ell) + \frac{(\mu\alpha + K\ell)^2}{2!} - \frac{(\mu\alpha + K\ell)^3}{3!} + \text{----------}$

if $(\mu\alpha + K\ell) << 1$ $\quad e^{-(\mu\alpha + K\ell)} \cong 1-(\mu\alpha + K\ell)$.

$$F_2 \cong F_1 (1 - \mu\alpha - K\ell) \text{ ----------(4)}$$

Therefore, as a rule of thumb, if $\mu\alpha + K\ell \leq 0.3$ then equation (4) can be used; if $\mu\alpha + K\ell > 0.3$ then equation (3) must be used. The values for μ and K depend on the type of steel used and the surface properties of the contact materials.

For practically all prestressed concrete structures, the depth is small compared with the length, so the

projected length of tendon measured along the axis of the member can be used when computing frictional losses. Similarly, the angular change α is given by the transverse deviation of the tendon divided by its projected length. (Both referred to the axis of the member.)

There are several different methods of overcoming the frictional loss in tendons. These methods will be discussed in the following paragraphs.

One method of overcoming the frictional loss is overtensioning the tendons. This method can be used when frictional loss is below 20 or 30 per cent of the prestressing force. The amount of overtension usually provided is equal to the maximum frictional loss.

Another method is to reduce the length of prestressing units. If the length of the prestressing units are large, as in Figure 22, losses in the prestressing force due to friction will be large. The frictional losses may be reduced by using shorter lengths of discontinuous steel with intermediate anchorages, as in Figure 23, instead of continuous steel with end anchorages only. Intermediate anchorages are generally subject to high stress concentrations and adequate reinforcement and additional prestressing is always necessary to prevent cracking. Figure 24 shows another arrangement in which the length of prestressing units may also be reduced by prestressing one span at a time. The beams are constructed

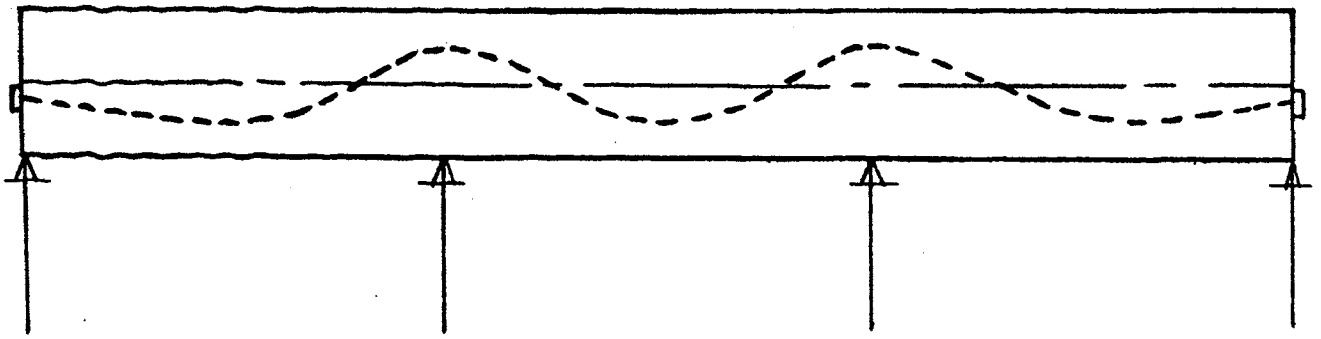

Fig. 22. Three-Span Prismatic Continuous Beam.

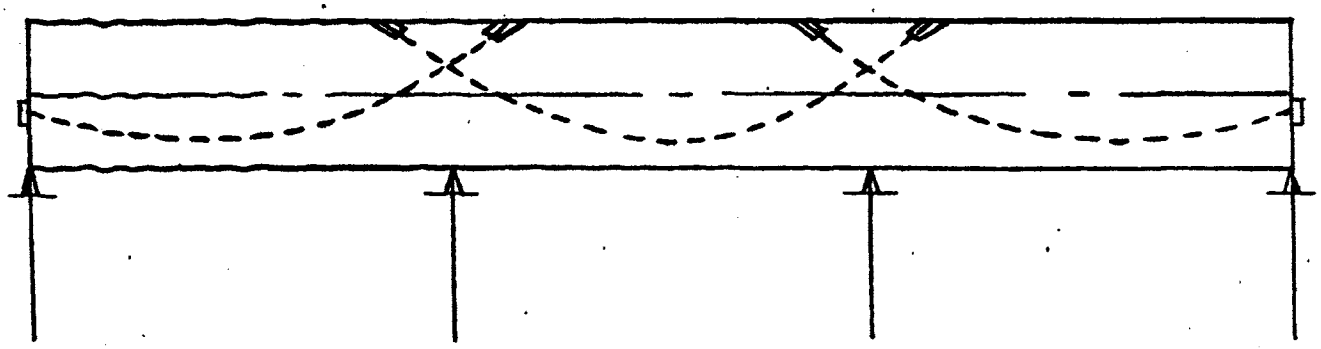

Fig. 23. Continuous Prestressed Concrete Beam with Intermediate Anchorages at the Top.

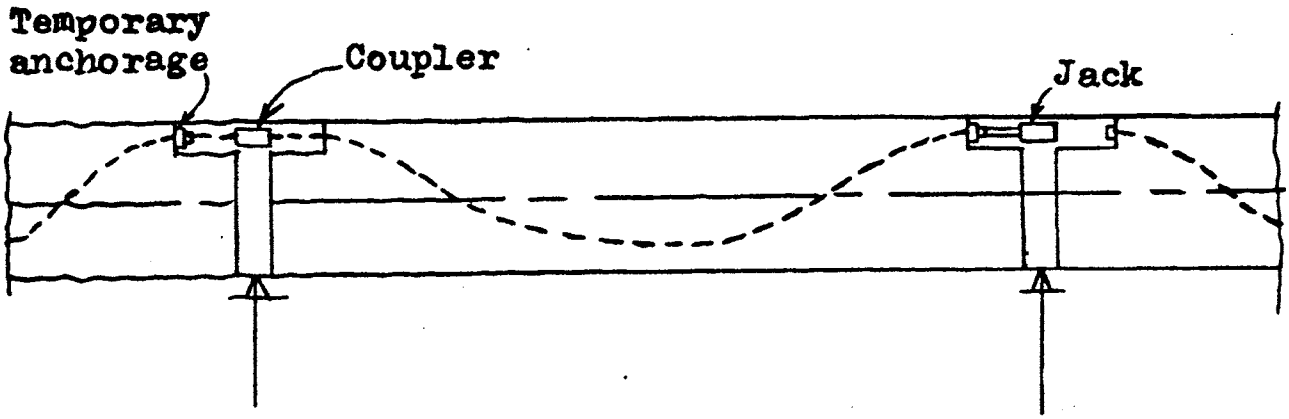

Fig. 24. Continuous Prestressed Concrete Beam Constructed in Parts from Left to Right.

individually from left to right. After the beam crossing one span is fully prestressed, the portion of the beam crossing the adjacent span is built, and its unstressed tendon is connected to the stressed tendon of the previous portion by a coupler. A jack is then applied to the right end for tensioning.

Reducing the curvature of the tendon is another method of overcoming friction loss. It is possible to eliminate the curvature entirely by using straight tendons and haunching the beam, as shown in Figure 25. The center of gravity line of the section becomes a curve, thus the desired eccentricities are obtained throughout the structure. However, it is difficult to control the eccentricity throughout the length of the structure in the construction, and from a practical point of view it seems to be satisfactory to use curved beams and slightly curved tendons at the same time as shown in Figure 26. This would permit a considerable reduction of the curvature of the profile of steel and avoid high frictional loss.

Reducing the coefficient of friction also reduces friction loss. The coefficient of friction varies greatly. It not only depends on the condition of the tendons at the time of prestressing and the material surrounding the prestressing tendons, but also depends a great deal on the care exercised in construction. By

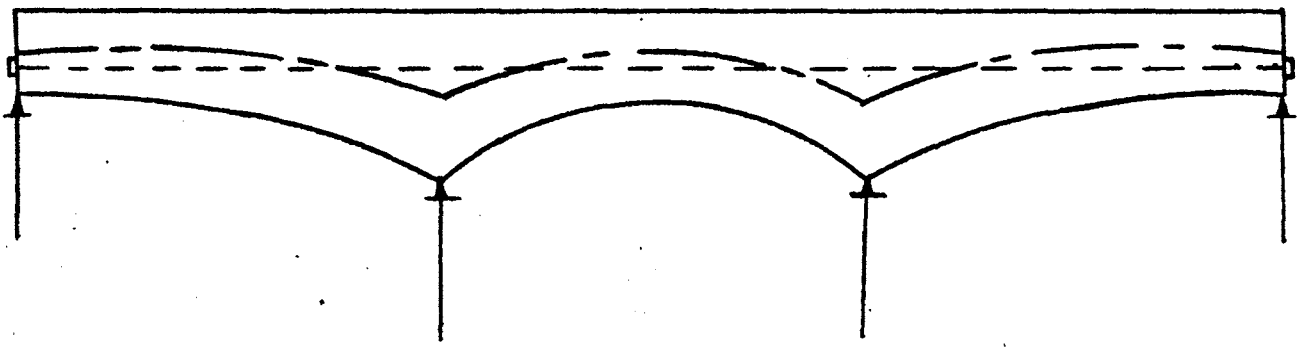

Fig. 25. Continuous Prestressed Concrete Beam with Variable Depth and Straight Prestressing Tendon.

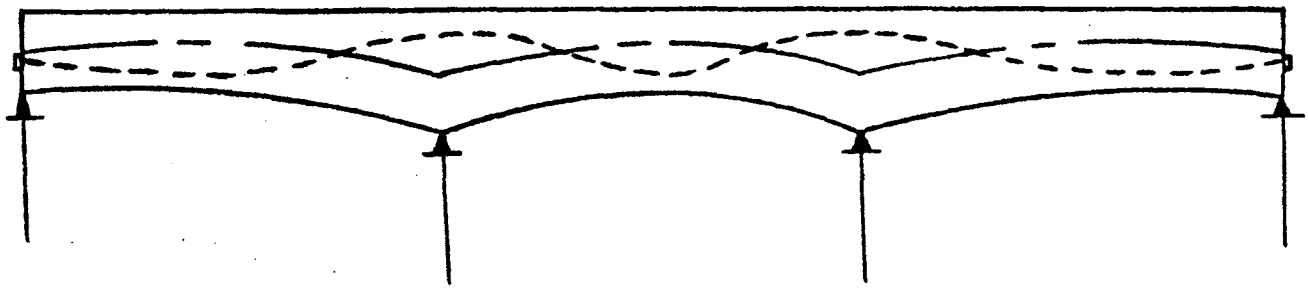

Fig. 26. Continuous Prestressed Concrete Beam with Variable Depth and Reduced Curvature of Prestressing Tendon.

the proper choice of materials and care in construction, it is possible to reduce the coefficient of friction to a very small quantity.

The last method considered is that of jacking from both ends. When the spans are long or when the angles of bending in tendons are large, jacking from both ends can be used to reduce frictional losses.

IV. DERIVATION OF EQUATIONS FOR CABLE GEOMETRY

In the design of continuous, prestressed concrete structures the most critical problem is the practical aspect of placing the tendons and the calculation of the fixed-end moments due to prestressing. Various cases of practical tendon profiles will be discussed in this section. The equations of the preceding chapter can be used to calculate the friction loss for all of the cable arrangements discussed below. It is assumed that the members are elastic and that deflections of the structure do not alter its dimensions for purposes of analysis.

In order to determine the upward pressure exerted on a stressed tendon which has a profile concave downward, a small section ds of the curved surface as shown in Figure 27 is analyzed.

A summation of forces in the vertical direction yields

$$dp = 2F\sin\frac{d\alpha}{2}$$

Since the angle $d\alpha$ is small,

$$dp = 2F\sin\frac{d\alpha}{2} \cong 2F\,\frac{d\alpha}{2} = Fd\alpha$$

The uniform upward pressure w_p resulting from the tendon force is

$$w_p = \frac{dp}{ds} = \frac{Fd\alpha}{ds} = F\,\frac{(1)}{\frac{ds}{d\alpha}} = F\,\frac{(1)}{R},$$

where R is the radius of curvature.

Therefore $F = Rw_p$ ----------(5)

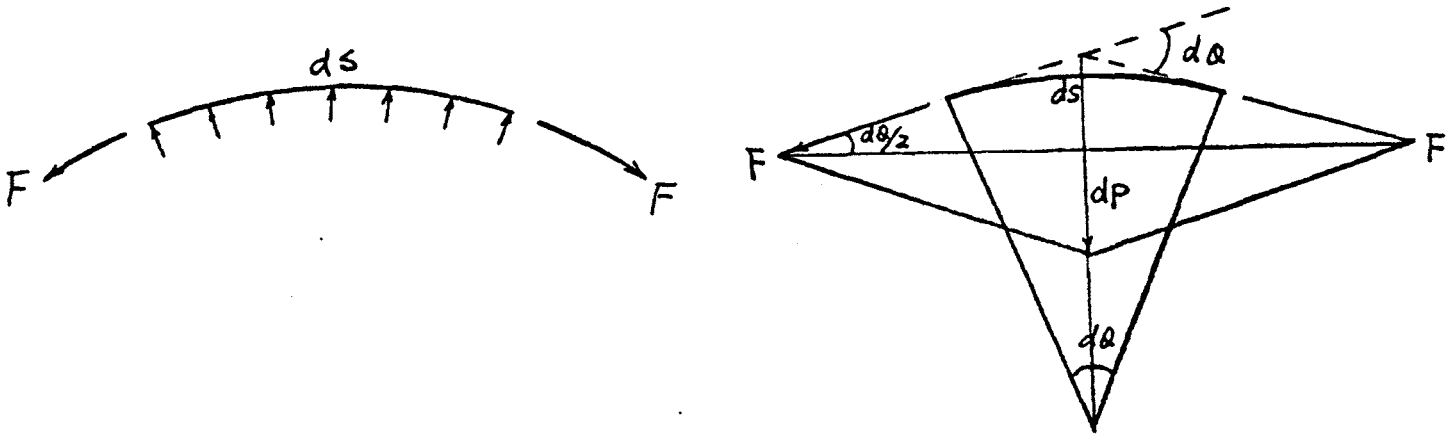

Fig. 27. Normal Forces Caused by Tendon in Contact with a Curved Surface.

A). Simple beam with end connections for post-tensioned tendons. For a very flat curve, points on a circle and on a parabola lie almost along the same curve. Figure 28 shows one-half of a beam with the end connections of the post-tensioned tendons at mid-depth and having a center line eccentricity of h. For this simple beam the post-stressed tendons are placed along the circular arc as shown. An expression can be derived for the radius of curvature in terms of the span length L and the center eccentricity h by use of the Pythagorian theorem, i.e.,

$$R^2 = (\frac{L}{2})^2 + (R - h)^2$$

from which

$$R = \frac{L^2}{8h} + \frac{h}{2} = \frac{L^2 + 4h^2}{8h}$$

Substituting $R = \frac{L^2 + 4h^2}{8h}$ in (5)

$$F = \frac{L^2 + 4h^2}{8h} w_p \text{ ----------(6)}$$

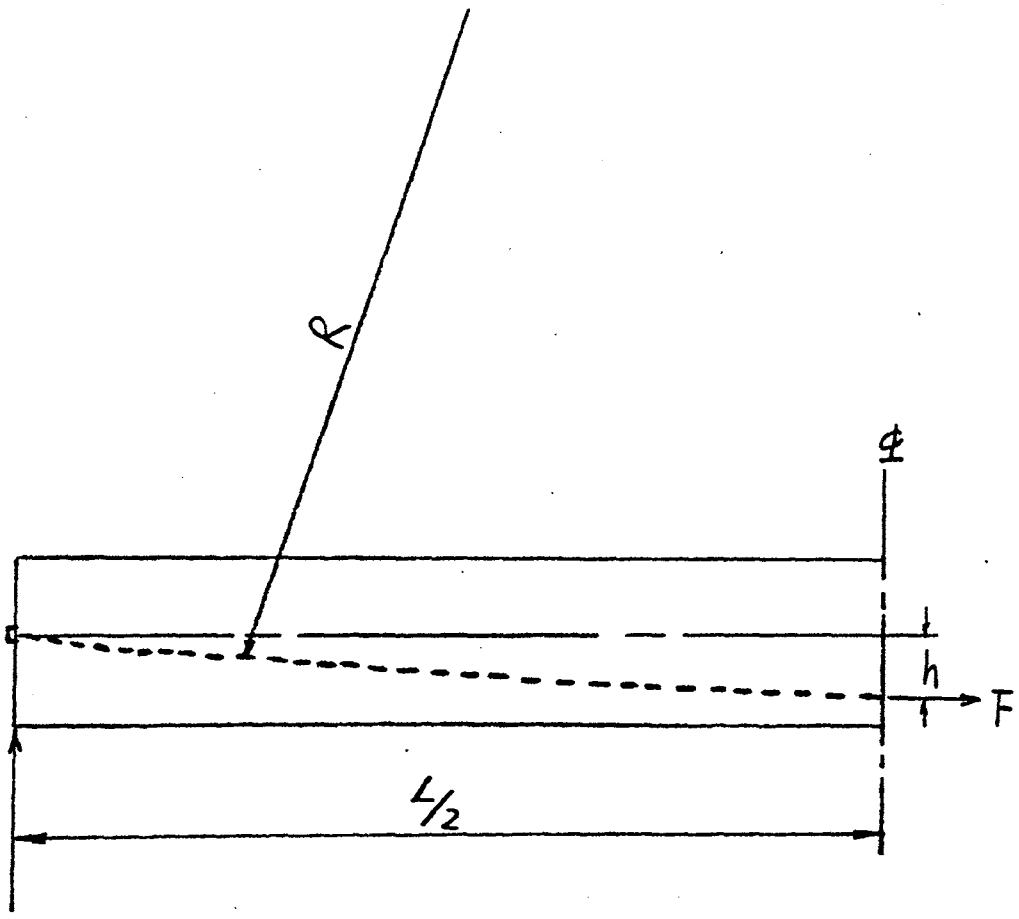

Fig. 28. Simple Beam with End Connections for Post-Tensioned Tendons.

B). Continuous beam with constant section and straight tendons. The continuous beam in Figure 29-a is of constant section with straight post-tensioned tendons. The structure may be analyzed as follows:

Consider support B to be removed and determine the displacement at B caused by prestress. The deflection (Figure 29-b) is

$$\delta_b = \frac{Fh(2\ell)^2}{8EI}$$

Then a reaction R_b is added as shown in Figure 29-c. This displacement may be expressed as

$$\delta'_b = \frac{R_b(2\ell)^3}{48EI}$$

The condition of no displacement at B is used to obtain an expression for R_b. That is,

$$\delta_b = \delta'_b$$

or $$\frac{Fh(2\ell)^2}{8EI} = \frac{R_b(2\ell)^3}{48EI}$$

from which

$$R_b = \frac{3Fh}{L} \text{ ----------(7)}$$

From statics,

$$R_a = R_c = \frac{3Fh}{L}\ (1/2) = \frac{3Fh}{2L}$$

and $M_b = R_a L - Fh = \frac{3Fh}{2L} (L) - Fh = \frac{Fh}{2}$

The bending moment diagram due to the prestressing force, F, is shown in Figure 29-d.

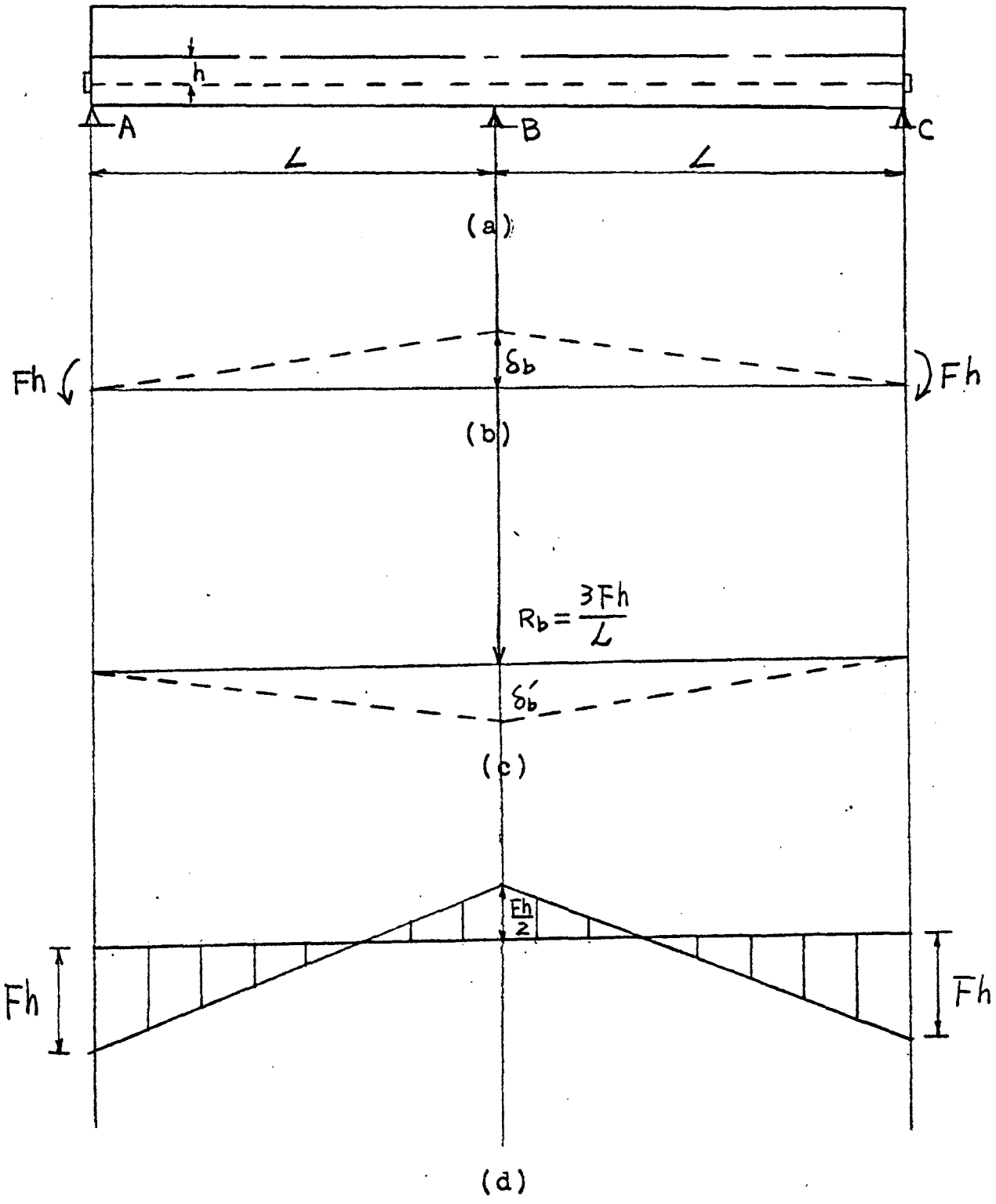

Fig. 29. Continuous Prestressed Concrete Beam with Constant Section and Straight Tendons.

C). Continuous beam with parabolic eccentricity and straight tendons. The continuous beam in Figure 30-a has straight prestressing tendons with the eccentricities of the end connections equal to zero. The cross section of the beam is constant but its axis is in the form of two parabolas. The midspan eccentricity is indicated as h.

Support B is removed and the bending moment diagram resulting from the post-tensioning moment is plotted as shown in Figure 30-b. The deflection at B for the simple span A-C may be derived as follows:

$$\frac{1}{2}\delta_B = \frac{1}{2}\left[\frac{(2/3)(Fh)\ell}{EI} \times \frac{3(2L)}{4}\right] - \frac{(2/3)(Fh)}{EI} \times \frac{\ell}{2}$$

$$= \frac{(2/3)(Fh)\ell}{EI}\left(\frac{3\ell}{4} - \frac{\ell}{2}\right) = \frac{(2/3)(Fh)\ell}{EI}\left(\frac{\ell}{4}\right)$$

$$\text{then } \delta_B = \left(\frac{\ell}{2}\right)\frac{(2/3)(Fh)\ell}{EI} \qquad \text{(upward)}$$

Now a reaction R_b is added, causing the bending moment diagram shown in Figure 30-c. Using the bending moment diagram, the deflection at B is

$$\delta'_B = \frac{1}{2}\left[\frac{1}{2}\left(\frac{R_bL}{2EI}\right)(2L)(L)\right] - \left[\left(\frac{R_bL}{2EI}\right)\left(\frac{L}{2}\right)\left(\frac{L}{3}\right)\right]$$

$$= \frac{R_b L^3}{4EI} - \frac{R_b L^3}{4EI}\left(\frac{1}{3}\right) = \left(\frac{2}{3}\right)\left(\frac{R_b L^3}{4EI}\right) \quad \text{(downward)}$$

The reaction R_b may be determined from the condition of $\delta_B = \delta_B'$, i.e.,

$$\left(\frac{L}{2}\right)\frac{(2/3)\,(Fh)L}{EI} = \left(\frac{2}{3}\right)\frac{R_b L^3}{4EI}$$

from which

$$R_b = \frac{2Fh}{L} \qquad \text{----------(3)}$$

since $w_p = \frac{8Fh}{L^2}$ (Equation 1) then $R_b = \frac{w_p L}{4}$

Now $M_b = \frac{1}{2}\left(\frac{w_p L}{4}\right)(L) = \frac{w_p L^2}{8}$

where M_b is the moment at B due to the prestressing force.

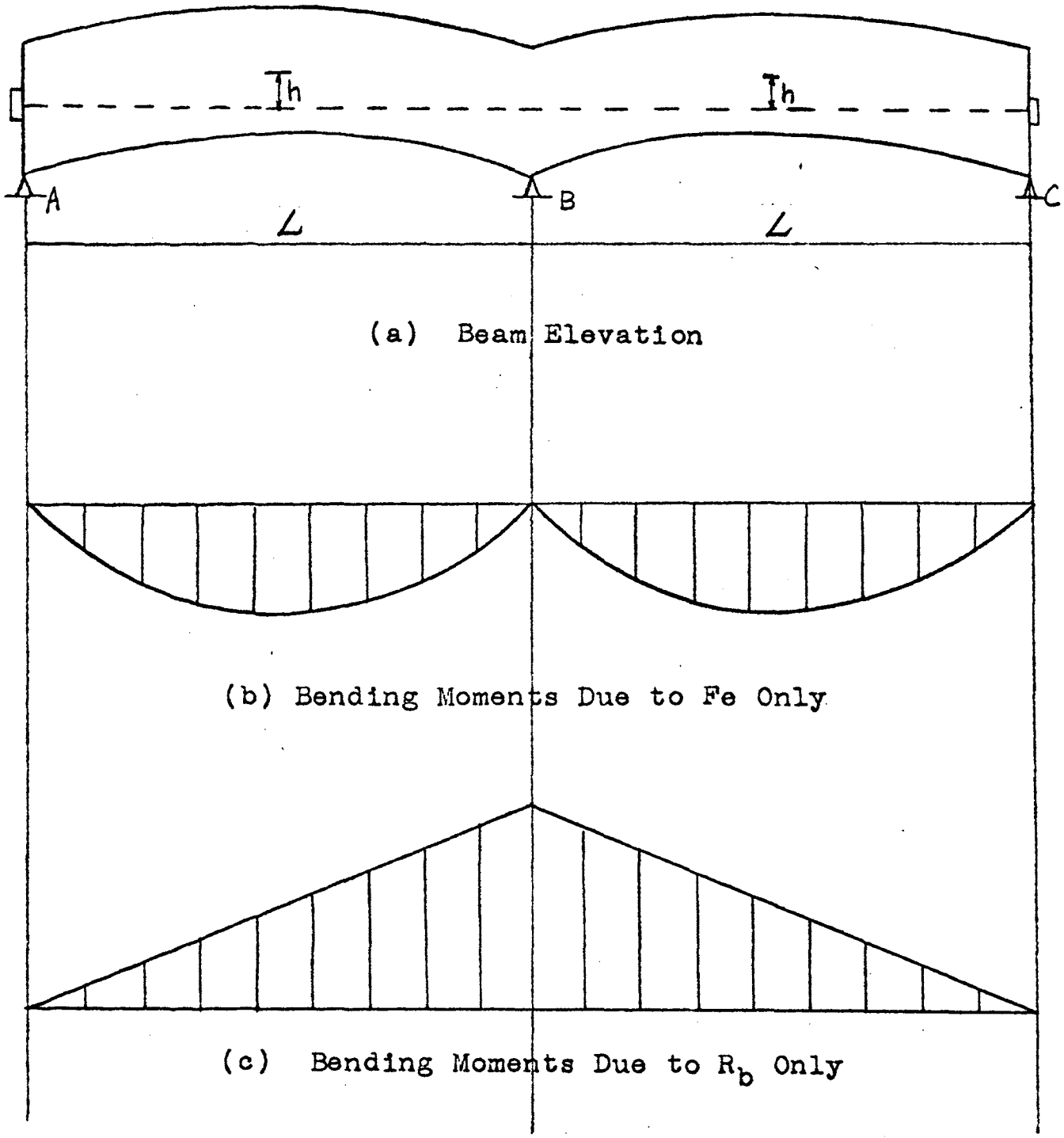

Fig. 30. Continuous Prestressed Concrete Beam with Variable Eccentricity and Straight Tendons.

D). Variable section, continuous, prestressed concrete beam with straight prestressing elements. A two-span continuous beam is shown in Figure 31-a. The end connections are at mid-depth and each midspan eccentricity is h. Consider the case where the upper side is straight, the lower side is curved parabolically, and the post-tensioning tendon is straight.

In Figure 31-b, if A_1 is the area of the M/EI_x diagram resulting from post-tensioning and if span A-B is assumed to be simple and disconnected from B-C, the change in slope at B is

$$\alpha'_B = \frac{A_1(L/2)}{L} = \frac{A_1}{2} = \int_0^L \frac{M_x dX}{2EI_X}$$

where

$$I_X = \frac{b}{12L^6}(4\delta X^2 - 4L\delta X + L^2d)^3 \text{ in span A-B;}$$

b and d mean the width and depth of the beam respectively.

$$M_x = \frac{w_p LX}{2} - \frac{w_p X^2}{2} = \frac{w_p(LX-X^2)}{2}$$

Substituting Mx into α'_B

$$\alpha'_B = \int_0^L \frac{w_p(LX-X^2)\,dX}{4EIx}$$

For a moment, M_B, applied at B, if a_1 is the area of the

M/EI diagram for M_2 equal unity, and $\bar{X}$ is the distance from A to the centroid of this area as shown in Figure 31-c, the change in slope at B due to M_B is

$$\alpha_B = \frac{\bar{X} M_B a_1}{L} = \frac{M_B}{L} \quad (\bar{X} a_1)$$

where $\bar{X} a_1 = \int_0^L X da_1 = \int_0^L x\left(\frac{M_x dx}{EI_x}\right) = \int_0^L X\left(\frac{(X/L)\, dX}{EI_x}\right)$

Now $\bar{X} a_1 = \int_0^L \frac{X^2 dX}{L EI_x}$

Substituting Xa_1 into α_B yields

$$\alpha_B = \frac{M_B}{L^2} \int_0^L \left(\frac{X^2 dX}{EI_x}\right)$$

The condition of no change in slope at B may be expressed as

$$\alpha_B = \alpha'_B$$

Therefore,

$$\frac{M_B}{L^2} \int_0^L \left(\frac{X^2 dX}{EI_x}\right) = \int_0^L \frac{w_p (LX - X^2) dX}{4EI_x}$$

which yields

$$M_B = \frac{\int_0^L \frac{w_p (LX - X^2) dX}{4EI_x}}{\int_0^L \frac{X^2 dX}{L^2 EI_x}} \qquad \text{----------(9)}$$

where M_B is the moment at B due to the prestress force.

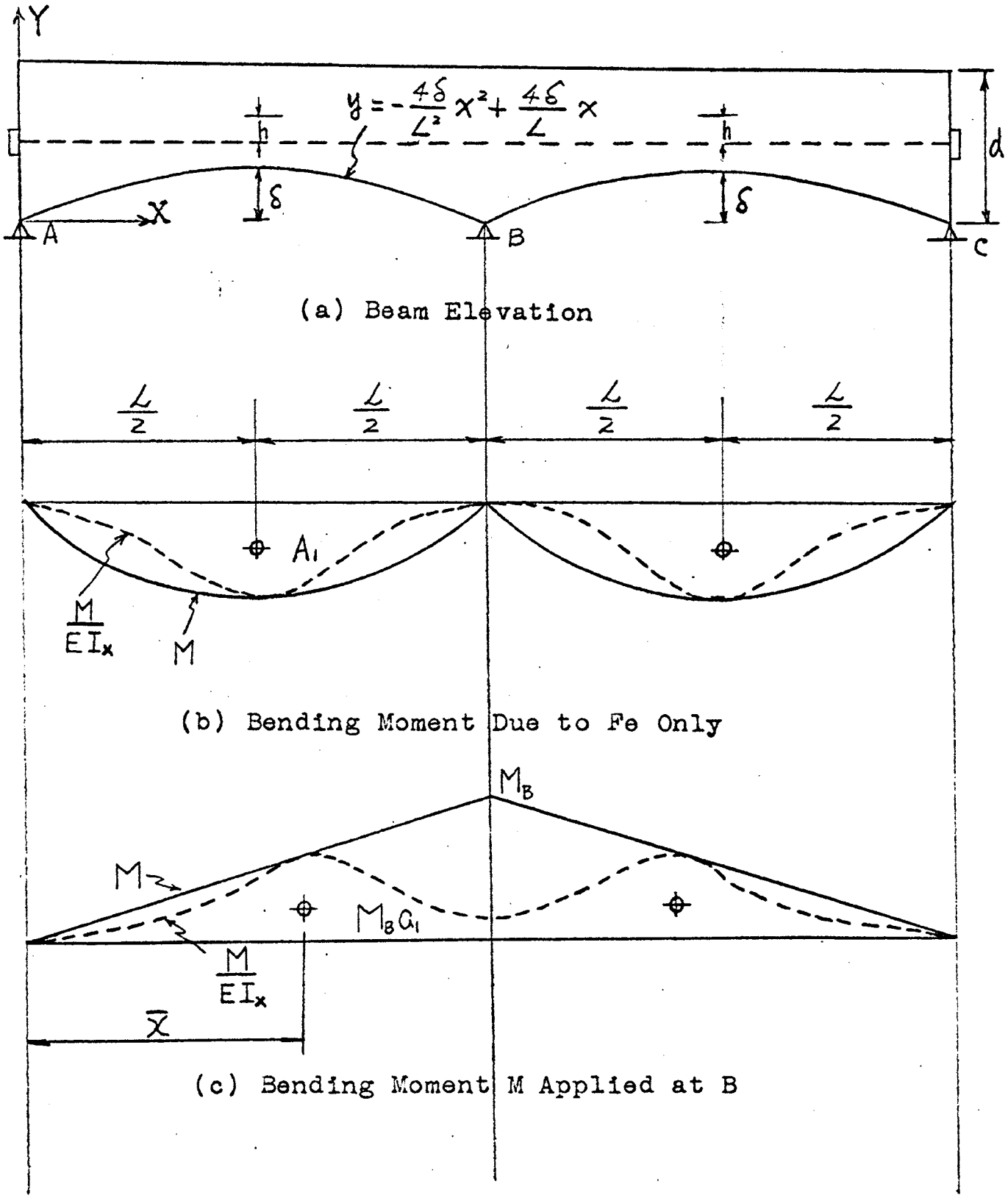

Fig. 31. Continuous Prestressed Concrete Beam with Variable Section and Straight Prestressing Tendons.

E). Constant section, continuous, prestressed concrete beam with curved tendons. It was pointed out previously that from a practical point of view, it is impossible to place the tendons in the configuration shown in Figure 3. Figure 4 shows the shapes of tendon curves in practice. It should be noted that tendons are placed in smooth curves. These curves are usually continuous parabolas which exert upward forces where concave upward, and downward forces where concave downward.

Figure 32 shows a tendon with a reversal of curvature in the span. Since the curve is continuous, the slopes at the point of intersection of the two curves must be equal. If the point of reversal is a distance b_1L from the support, then it is seen from the properties of a parabola that the distance $d_1 = d_1'$ and $d_2 = d_2'$. Since triangles PRV and TRS are similar as are triangles VRW and VSU,

$$\frac{2d_1}{b_1L} = \frac{2d_2}{b_2L} \quad \text{and} \quad \frac{2d_1}{b_1L} = \frac{2d}{L/2}.$$

Therefore, $d_1 = 2db_1$, $d_2 = 2db_2$.

From the above relation, the forces exerted by the tendon on the concrete may be derived as follows:

$$Fd_1 = \frac{w_1(2b_1L)^2}{8} \text{(downward) and } Fd_1 = \frac{w_2(2b_2L)^2}{8}$$

(upward).

Therefore,

$$w_1 = \frac{2Fd_1}{b_1^2L^2} \quad \text{and} \quad w_2 = \frac{2Fd_2}{b_2^2L^2}$$

Substituting d_1 and d_2 into w_1 and w_2 yields

$$w_1 = \frac{2F(2db_1)}{b_1^2L^2} = \frac{4Fd}{b_1L^2} \quad \text{(downward)} \text{----------} (10)$$

$$w_2 = \frac{2F(2db_2)}{b_2^2L^2} = \frac{4Fd}{b_2L^2} \quad \text{(upward)} \text{----------} (11)$$

For the special case in which $b_2 = 0.5$, $w_2 = \frac{8Fd}{L^2}$, which is the same equation that was derived for a simple hung cable (Equation 1).

Using the above equations, the tendon force, F, can be converted into equivalent uniformly distributed loads on the structure which makes it possible to compute the fixed-end moments.

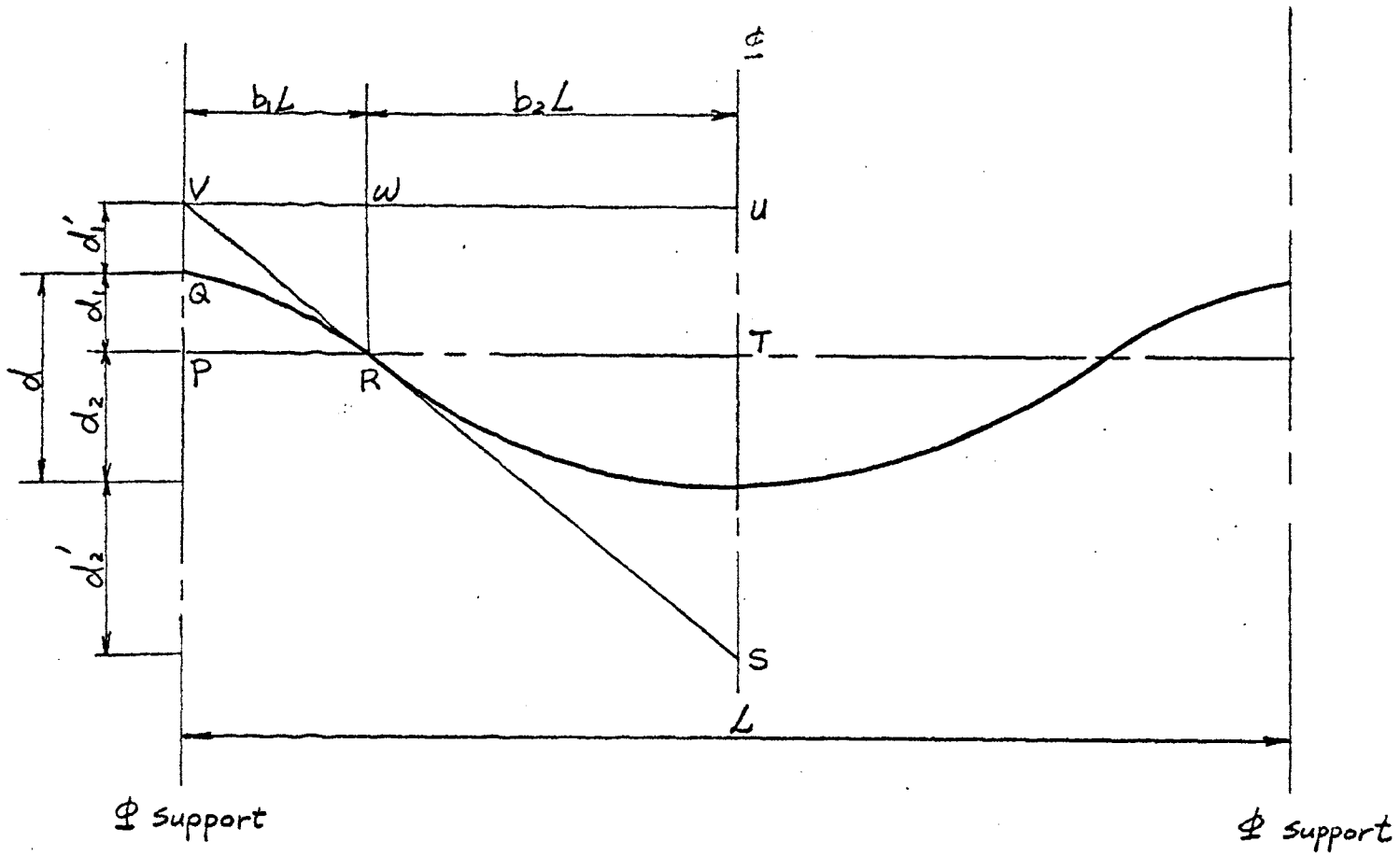

Fig. 32. A Prestressing Tendon with a Reversal of Curvature in the Span.

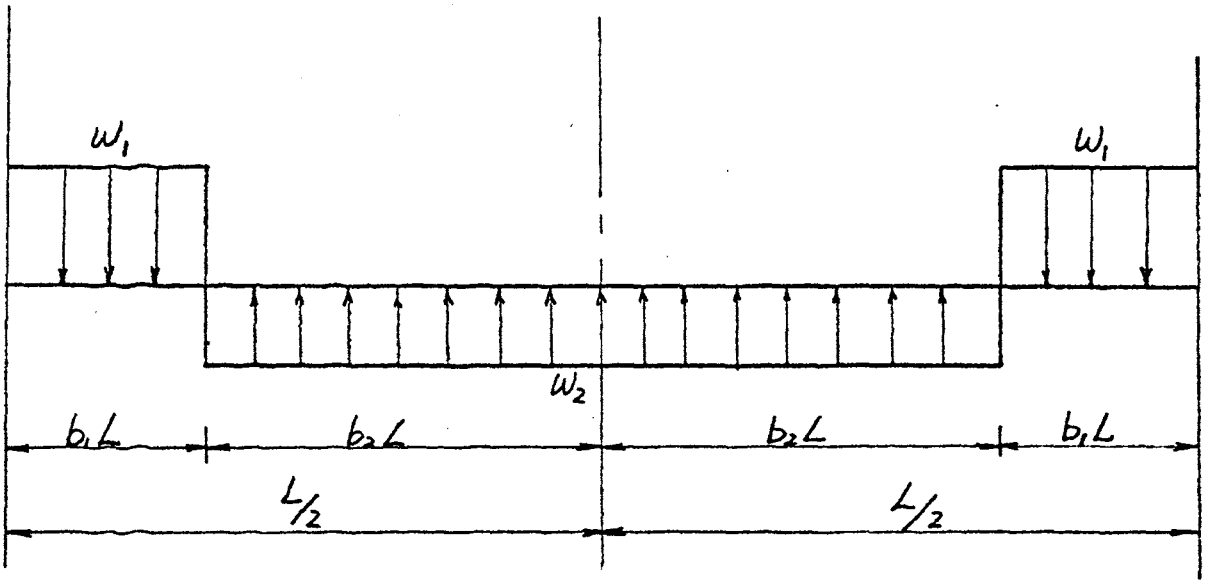

Fig. 33. Loading Diagram due to Prestress Fig. 32.

V. DESIGN CHARTS FOR FIXED-END MOMENT

The calculation of fixed-end moments due to the prestressing force using the formulas derived in the preceding section is quite cumbersome. In order to simplify the calculations, design charts for fixed-end moments will be developed in this section.

The parabolic tendon in Figure 32 is symmetrical about the center line of the span and has a total drape "d". In this case, the fixed-end moments can be determined by loading the span with the upward and the downward loads w_1 and w_2 as shown in Figure 33.

By separating the loading condition of Figure 33 into two parts as shown in Figure 34-a and Figure 34-b, and assuming EI is uniform, the fixed-end moment equations in terms of F, d and b_1 may be derived as follows:
For the loading condition shown in Figure 34-a,

$$M_{1AB} = \frac{Fd}{3b_1}$$, where M_{1AB} is the moment due to the load w_1.

For the loading condition shown in Figure 34-b,

$$M_{2AB} = \frac{Fd}{3}(1 + 2b_1 - 2b_1^2)\left(\frac{1}{b_1} + \frac{1}{\frac{1}{2}-b_1}\right)(1-2b_1)$$

where M_{2AB} is the moment due to the loads w_1 plus w_2.
The equation for moment equilibrium at A is

$$M_{AB} = M_{2AB} - M_{1AB}$$

Therefore

$$M_{AB} = \frac{Fd}{3}(1 + 2b_1 - 2b_1^2)\left(\frac{1}{b_1} + \frac{1}{\frac{1}{2}-b_1}\right)(1-2b_1) - \frac{Fd}{3b_1}$$

$$= \left[\frac{1}{3}(1 + 2b_1 - 2b_1^2)\left(\frac{1}{b_1} + \frac{1}{\frac{1}{2}-b_1}\right)(1-2b_1) - \frac{1}{3b_1}\right]Fd.$$

or $M_{AB} = k(Fd)$ ----------(12)

where $k = \left[\frac{1}{3}(1 + 2b_1 - 2b_1^2)\left(\frac{1}{b_1} + \frac{1}{\frac{1}{2}-b_1}\right)(1-2b_1) - \frac{1}{3b_1}\right]$

It is seen that the fixed-end moment coefficient, k, depends only on b_1. Chart I shows values of the fixed-end moment coefficient, k, for a range of values of b_1. This chart is only valid for beams which are symmetrical about their center line. Figure 35 illustrates a tendon profile for an interior span. If $b_1 = 0.20$, the fixed-end moment is computed as follows:

From Chart I it is seen that k = 0.533; therefore,

$$M = k(Fd) = (0.533)(0.5)F = (0.2664)F = 0.2664F$$

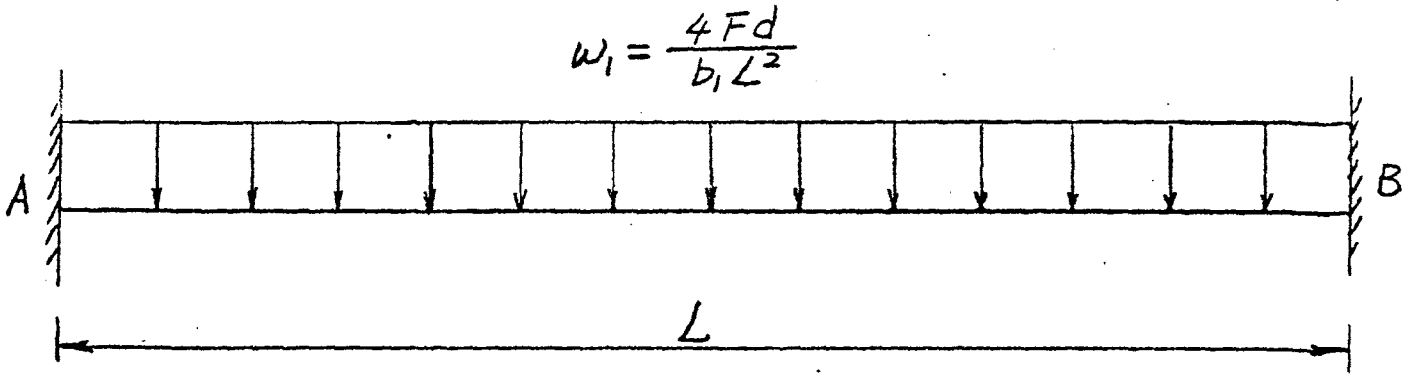

Fig. 34. (a)

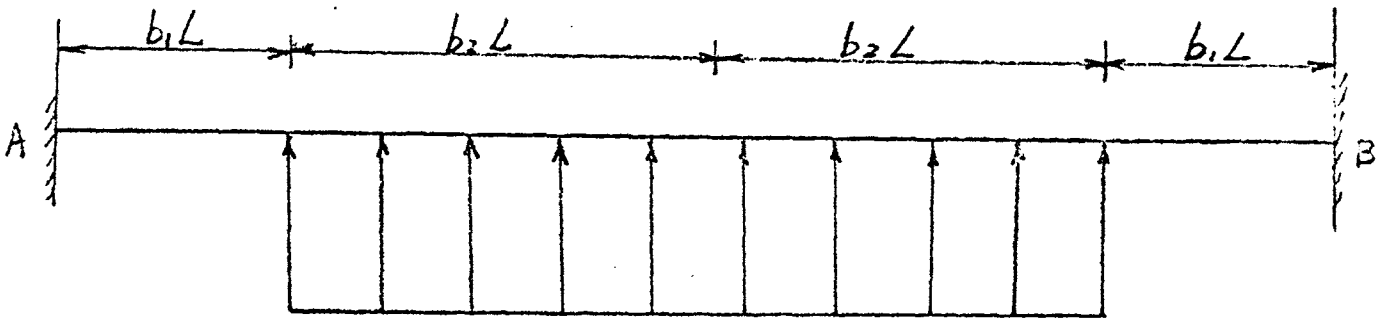

$$w_3 = w_1 + w_2 = \frac{4Fd}{b_1L^2} + \frac{4Fd}{b_2L^2}$$

(b)

Fig. 34. Separating Loading Condition of Figure 33.

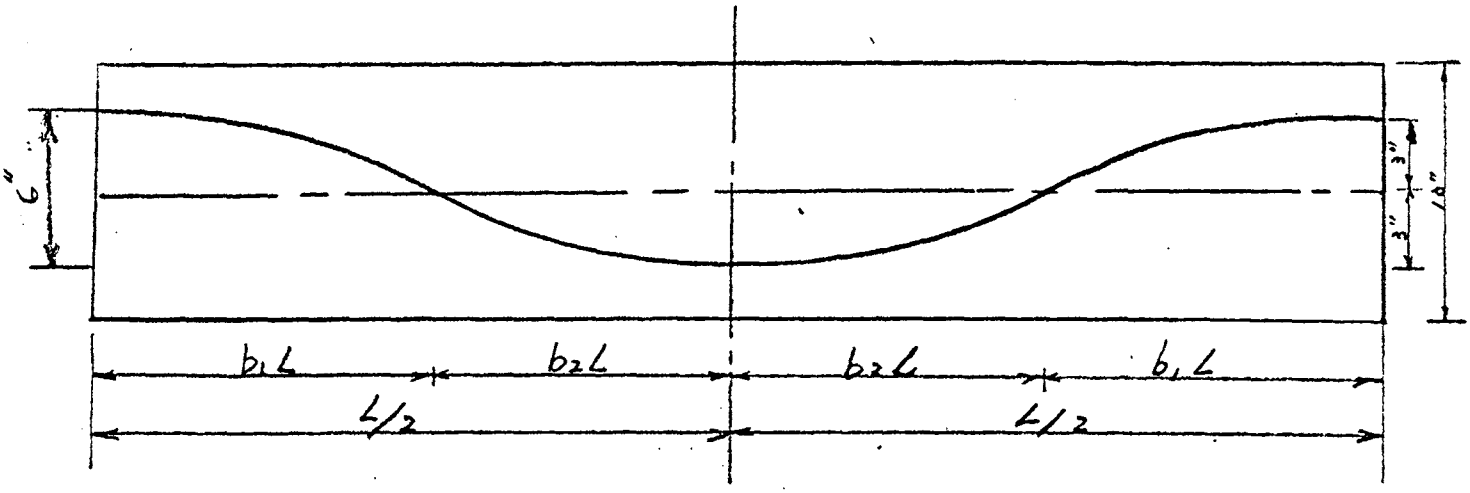

Fig. 35. A Tendon Profile for an Interior Span.

Since all tendons are not placed symmetrically, an unsymmetrical profile of tendons needs to be discussed. In Figure 36-a, the tendon consists of four portions of parabolic curves. For this span the prestressing produces

four uniform loads of different magnitudes as shown in Figure 36-b. The fixed-end moments can be calculated as follows:

The first step is to separate the loads into two parts as shown in Figure 36-c and Figure 36-d. Again divide the loads of Figure 36-c, into two parts as shown in Figure 36-e and Figure 36-f. The following are the fixed-end moments,

$$M_{3AB} = \frac{b_1^2(6-8b_1+3b_1^2)}{12}(w_1+w_2)L^2$$

$$= \frac{b_1^2}{3}(6-3b_1+3b_1^2)\left(\frac{1}{b_1}+\frac{1}{\frac{1}{2}-b_1}\right)Fa_1$$

or $$M_{3BA} = \frac{b_1^3(4-3b_1)}{12}(w_1+w_2)L^2$$

$$= \frac{b_1^3}{3}(4-3b_1)\left(\frac{1}{b_1}+\frac{1}{\frac{1}{2}-b_1}\right)Fa_1$$

$$M_{4AB} = \frac{11}{192}w_2L^2 = \frac{11}{192}\frac{(4Fa_1)}{\frac{1}{2}-b_1}$$

$$M_{4BA} = \frac{5}{192}w_2L^2 = \frac{5}{195}\left(\frac{4Fa_1}{\frac{1}{2}-b_1}\right)$$

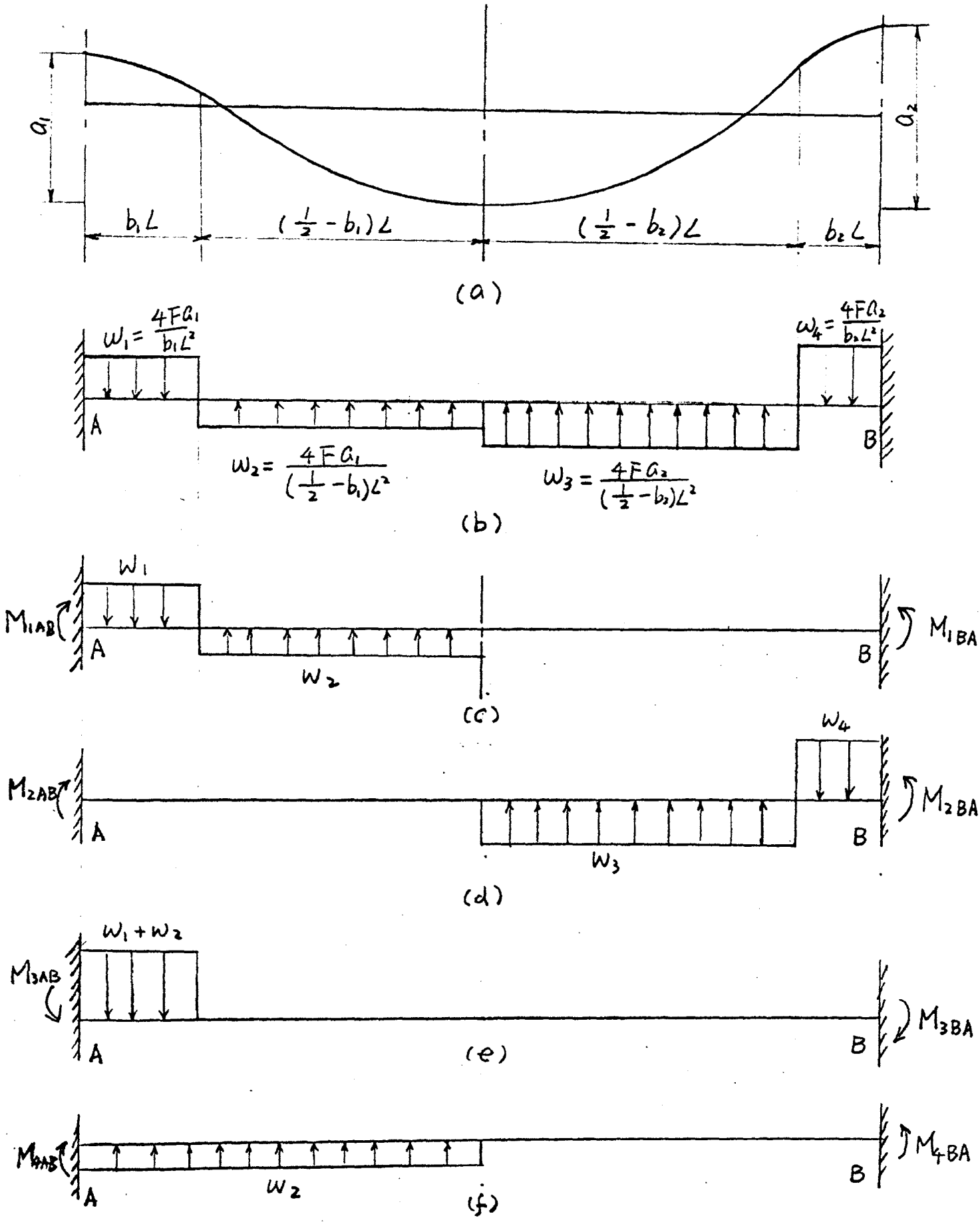

Fig. 36. Loading Condition for Chart II.

The two cases are combined as follows to find the fixed-end moment for the loading condition shown in Figure 36-c:

$M_{1AB} = M_{4AB} - M_{3AB}$ and $M_{1BA} = M_{4BA} - M_{3BA}$, that is:

$$M_{1AB} = \left[\frac{11}{192}\left(\frac{4}{\frac{1}{2}-b_1}\right) - \frac{b_1^2}{3}(6-8b_1+3b_1^2)\left(\frac{1}{b_1}+\frac{1}{\frac{1}{2}-b_1}\right)\right]Fa_1$$

$$= k_1 Fa_1 \text{----------(13)}$$

$$M_{1BA} = \left[\frac{5}{192}\left(\frac{4}{\frac{1}{2}-b_1}\right) - \frac{b_1^3}{3}(4-3b_1)\left(\frac{1}{b_1}+\frac{1}{\frac{1}{2}-b_1}\right)\right]Fa_1$$

$$= k_1' Fa_1 \text{----------(14)}$$

In the same manner the fixed end moments are determined for the loading condition shown in Figure 36-d. These moments are:

$$M_{2AB} = \left[\frac{5}{192}\left(\frac{4}{\frac{1}{2}-b_2}\right) - \frac{b_2^3}{3}(4-3b_2)\left(\frac{1}{b_2}+\frac{1}{\frac{1}{2}-b_2}\right)\right]Fa_2$$

$$= k_2 Fa_2 \text{----------(15)}$$

$$M_{2BA} = \left[\frac{11}{192} \left(\frac{4}{\frac{1}{2}-b_2}\right) - \frac{b_2^2}{3} (6-8b_2 - 3b_2^2)\left(\frac{1}{b_2} + \frac{1}{\frac{1}{2}-b_2}\right) \right] Fa_2$$

$$= k_2' Fa_2 \text{ ----------(16)}$$

where:

$$k_1 = \left[\frac{11}{192}\left(\frac{4}{\frac{1}{2}-b_1}\right) - \frac{b_1^2}{3}(6-8b_1 - 3b_1^2)\left(\frac{1}{b_1} + \frac{1}{\frac{1}{2}-b_1}\right)\right]$$

$$k_1' = \left[\frac{5}{192}\left(\frac{4}{\frac{1}{2}-b_1}\right) - \frac{b_1^3}{3} (4 - 3b_1) \left(\frac{1}{b_1} + \frac{1}{\frac{1}{2}-b_1}\right)\right]$$

$$k_2 = \left[\frac{5}{192} \left(\frac{4}{\frac{1}{2}-b_2}\right) - \frac{b_2^3}{3} (4 - 3b_2)\left(\frac{1}{b_2} + \frac{1}{\frac{1}{2}-b_2}\right)\right]$$

$$k_2' = \left[\frac{11}{192} \left(\frac{4}{\frac{1}{2}-b_2}\right) - \frac{b_2^2}{3} (6 - 8b_2 - 3b_2^2)\left(\frac{1}{b_2} + \frac{1}{\frac{1}{2}-b_2}\right)\right]$$

The resulting fixed-end moments for the cable profile shown in Figure 36-a are found by combining equations (13) and (15) and equations (14) and (16), i.e.,

$$M_{AB} = (k_1 a_1 + k_2 a_2) F \text{ ----------(17)}$$

and $$M_{BA} = (k_1' a_1 + k_2' a_2) F \text{ ----------(18)}$$

According to equations (17) and (18), Design Chart II is developed. The fixed-end moments can be computed by

using this chart, which gives values for fixed-end moment coefficients. To illustrate the use of the design charts, assume $b_1 = 0.15$, $b_2 = 0.20$, $a_1 = 4$ in., $a_2 = 6$ in. and F = 250 k. Then the fixed-end moments at A and B are computed as follows:

From Chart II it is seen that $k_1 = 0.307$, $k_2 = 0.259$, $k'_1 = 0.271$, $k'_2 = 0.262$.

Therefore,

$$M_{AB} = (k_1 a_1 + K_2 a_2)F$$

$$= \left[(0.307)\left(\frac{4}{12}\right) + (0.259)\left(\frac{6}{12}\right)\right](250)$$

$$= 57.75 \text{ k-ft.}$$

$$M_{BA} = (k_1' a_1 + k_2' a_2)F$$

$$= \left[(0.271)\left(\frac{4}{12}\right) + (0.262)\left(\frac{6}{12}\right)\right](250)$$

$$= 55.25 \text{ k-ft.}$$

In this analysis it was assumed that the cable was in a profile which was a series of parabolas. This method could be used without too much loss of accuracy if the profile is a series of circular segments.

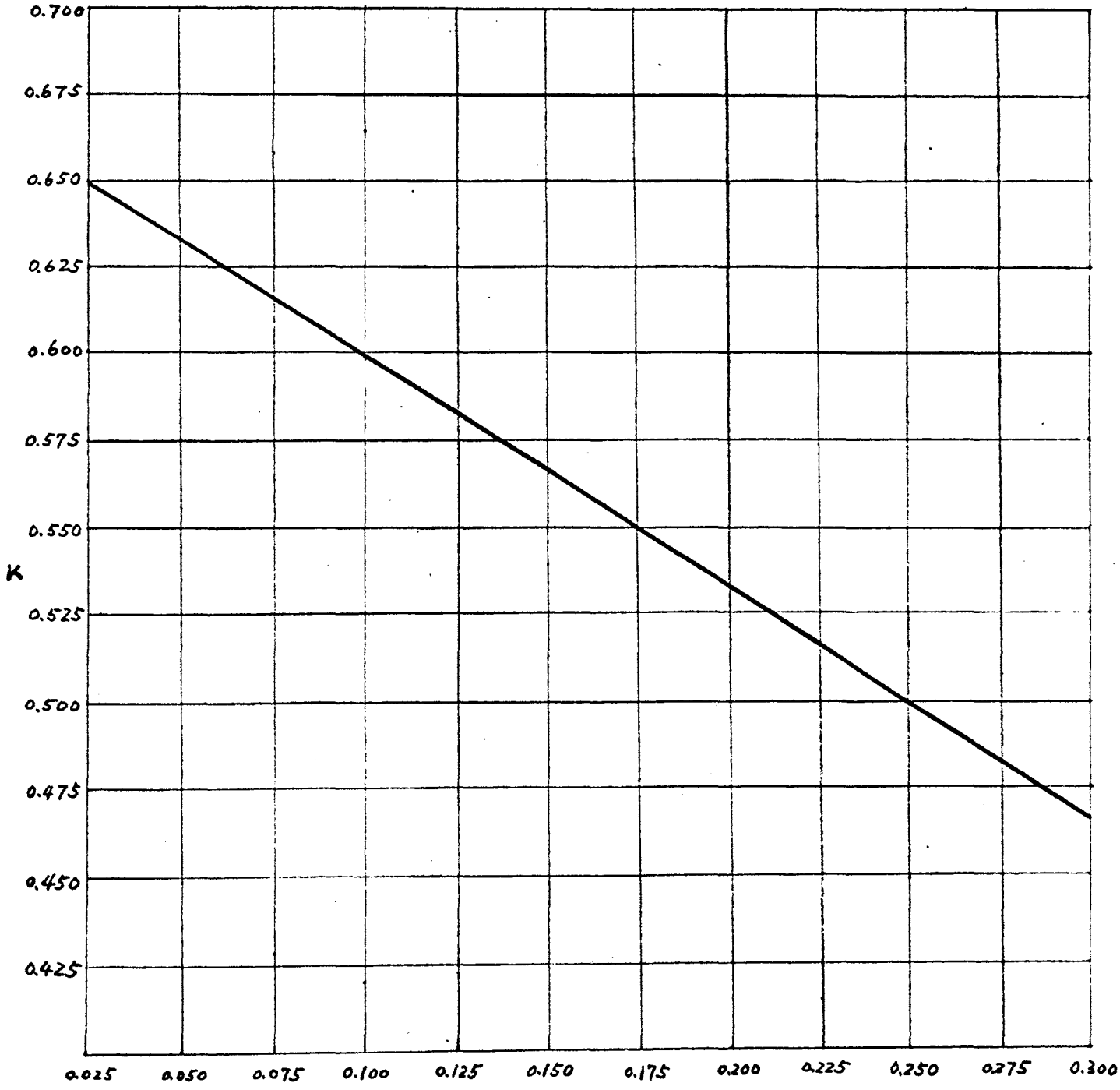

CHART I.

Moment Coefficients for a Symmetrical Cable Profile.

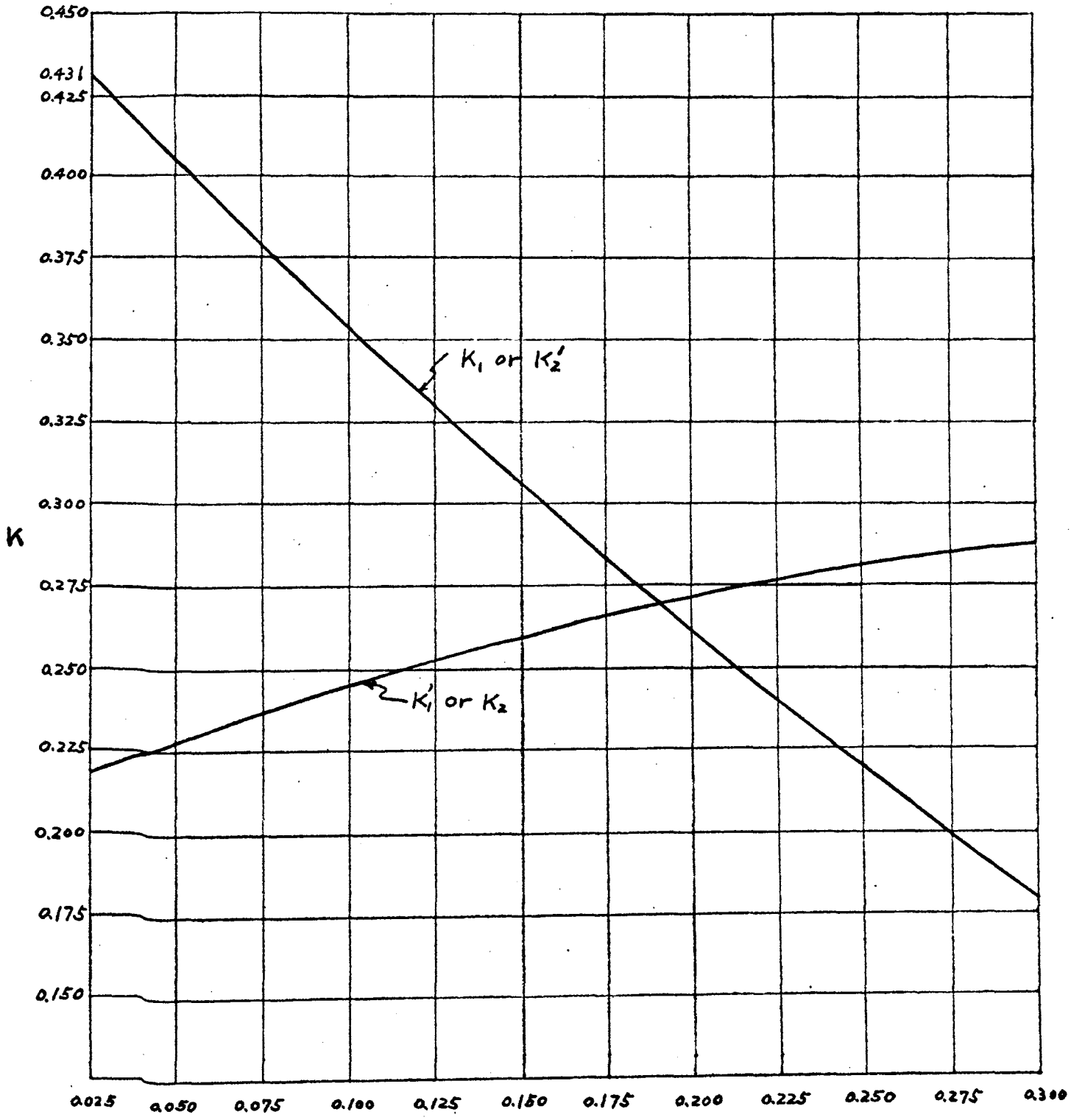

CHART II.

Moment Coefficients for an Unsymmetrical Cable Profile.

VI. THE EFFECT OF REVERSE CURVATURE

The design charts developed in Chapter V will be used in the analysis of a cable with reverse curvature as shown in Figure 37. In order to compare results, the cable has the same span and maximum eccentricity as the idealized cable analyzed previously in Section III. The points of reverse curvature were chosen at 0.10L from the center line of the supports.

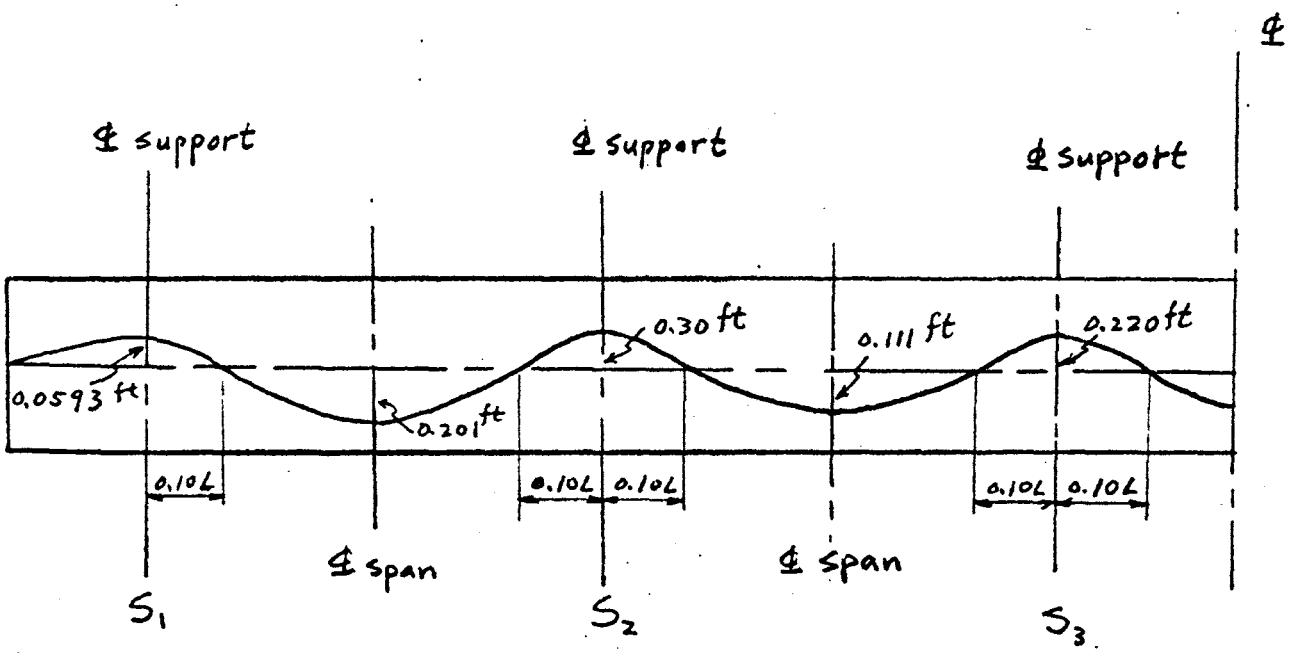

Fig. 37. Example of The Effect of Reverse Tendon Curvature of the Tendons.

The fixed-end moment coefficients are found in Chart II. Then the fixed-end moments are calculated as follows using Equations 17 and 18.

$$M_{s_1R} = \left[(0.3548)(0.0593+0.201)+(0.2446)(0.201+0.30)\right] F$$

$$= 0.215F$$

$$M_{s_2L} = \left[(0.2446)(0.0593+0.201)+(0.3548)(0.201+0.30)\right] F$$

$$= 0.241F$$

$$M_{s_2R} = \left[(0.3548)(0.30+0.111)+(0.2446)(0.111+0.220)\right] F$$

$$= 0.227F$$

$$M_{s_3L} = \left[(0.2446)(0.30+0.111)+(0.3548)(0.111+0.220)\right] F$$

$$= 0.218F$$

where the subscripts R and L refer to locations immediately to the right or left of the indicated support. The balanced fixed-end moments are shown in Figure 38.

	1		2		3	
	5 ft	25 ft		25 ft		25 ft
	0	1	½	½	½	½
F.E.M	−0.059F	+0.215F	−0.241F	+0.227F	−0.218F	+0.218F
1 − D	0	−0.156F	+0.007F	+0.007F	0	0
1 − CO.		+0.004F	−0.078F	0	+0.004F	−0.004F
2 − D	0	−0.004F	+0.039F	+0.039F	0	0
2 − CO		+0.020F	−0.002F	0	+0.020F	−0.020F
3 − D	0	−0.020F	+0.001F	+0.001F	0	0
3 − CO.		+0.001F	−0.010F	0	+0.001F	−0.001F
4 − D	0	−0.001F	+0.050F	+0.005F	0	0
Σ	−0.059F	+0.059F	−0.279F	+0.279F	−0.193F	+0.193F

Fig. 38. Balanced Fixed-end Moments for Fig. 37.

In simple structures, the moment due to the prestressing is always Fe, and the physical position of the tendon is always coincident with the line of thrust. In a continuous structure this is not necessarily true. The line of thrust can be moved up or down depending on the effect of continuity. It is seen that the moment at the

second support is 0.279F. Since this moment equals Fe' where e' is the distance of the line of thrust from the centroid of the cross-section, then 0.279F = Fe'. Thus, e' = 0.279 foot, whereas the actual physical location of the tendon is 0.300 foot. The location of the line of thrust at any position in the span can be found by dividing the moment by the prestressing force. At the second support, the secondary moment is (0.300F-0.279F) = 0.021F, since the secondary moments are defined as the difference between the resulting moment, Fe', and the primary moment, Fe.(1)

In Figure 11, it was assumed that there was no point of reversal, but in Figure 38 the reversal of curvature was considered. The two cases are compared in Figure 39. The differences are quite large especially if b_1 is large. The differences become larger since the differences are proportional to b_1. Usually the value of b_1 is between 0.10 and 0.150.

By this comparison, it can be seen that the effect of reversal of curvature must be considered in order to obtain a more economical design.

Support	1	2	3
Moment with reverse curvature (Figure 38)	0.059F	0.279F	0.193F
Moment without reverse curvature (Figure 11)	0.059F	0.300F	0.220F
Difference	0	0.021F	0.027F
% Error	0	7.5%	14%

Fig. 39. The Effect of Reverse Curvature.

VII. CONCLUSIONS

The results of this investigation have led to several conclusions, which follow:

1. The principal advantage of continuous prestressed concrete structures over conventionally reinforced structures is that the amount of the dead load moments can be eliminated or controlled very precisely by varying the prestressing force. Hence it is possible to use a smaller depth for a continuous structure without decreasing its stiffness.

2. In simple or statically determinate structures, the physical position of the tendon is always coincident with the line of thrust when there is no dead load or live load on the beam. In a continuous structure this is not necessarily true, since the line of thrust can be moved up or down depending on the effect of continuity.

3. In order to make the moments due to the prestressing force opposite to those caused by the acting loads, the prestressing force must act below the centroid of the cross-section in the center of each span, while over the supports it must act above the centroid. In order to satisfy this condition, the profile of the center of gravity of steel has to have a varying curvature as it passes from a region of positive moment to a support.

The effect of reversal of curvature is quite large (14 to 20 percent) and must be considered in order to obtain a more economical design.

4. The charts developed in this thesis greatly simplify the calculation of fixed-end moments due to prestressing force, and a rapid design can be made.

5. The effect of the reversal of curvature varies directly with b_1 (See Figure 36-a). If b_1 increases, the effect of the reversal of curvature becomes larger. Similarly, if b_1 decreases, the effect of the reversal of curvature becomes smaller. If b_1 is less than 0.05, the cable under consideration may be treated as an idealized cable with very little loss of accuracy.

BIBLIOGRAPHY

1. LIN, T.Y., (1963). Design of Prestressed Concrete Structures. Wiley Company, New York. p. 300-338.

2. CHI, MICHAEL and BIBERSTEIN, FRANK A. (1963). Theory of Prestressed Concrete. Prentice-Hall, Inc., New Jersey, p. 83-105.

3. KHACHATURIAN, NARBEY (1962). Service Load Design of Prestressed Concrete Beam Part III Continuous Beams. University of Illinois. Distributed by the Illini Union Bookstore.

4. FARMER, L.E. (1965). Prestressed Concrete Design. Notes from Class. The University of Missouri at Rolla, Rolla, Missouri.

5. GUYON, Y. (1960). Prestressed Concrete. Wiley Company, New York, Vol. II, p. 1-129.

6. LIN, T.Y. and ITAYA R. (1958). Behavoir of A Continuous Concrete Slab Prestressed in Two Directions. University of California. Paper 100, p. 22-27.

7. OZELL, A.M. (1957). Behavior of Simple-Span and Continuous Composite Prestressed Concrete Beams. Prestressed Concrete Institute, Vol. 2, No. 1, p. 45-76.

8. DUNHAM, CLARENCE W. (1964). Advanced Reinforced Concrete. McGraw-Hill Company, New York, p. 174-177.

VITA

Ping-Chi Mao, the son of Mr. and Mrs. Dah-Ruey Mao, was born on May 2, 1934, at Taiwan, China. He received his grade and high school education at Kaohsiung in Taiwan. He entered Cheng-Kung University in September, 1955, and graduated in June, 1959, with a B. S. C. E.

After graduating, he was employed as a junior engineer at the Taiwan Public Works Bureau for one year. The next three years were spent at Kaohsiung Senior Girls' High School and Kaohsiung Senior Technical School, as a mathematics and structural theory teacher respectively.

He was married to Miss Hsueh-Li Hong on August 6, 1961. They have one boy, Wei-Jen, who was born November 6, 1963.

In January, 1964, he enrolled in the University of Missouri at Rolla to work towards the degree of Master of Science in Civil Engineering.